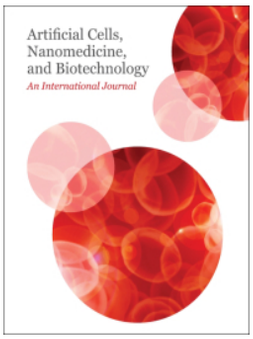

Taylor & Francis
Taylor & Francis Group

Artificial Cells, Nanomedicine, and Biotechnology
An International Journal

ISSN: 2169-1401 (Print) 2169-141X (Online) Journal homepage: www.tandfonline.com/journals/ianb20

Preliminary genipin-crosslinked gelatin–asiaticoside injectable hydrogel for future biomaterials ink: physicochemical properties and cytocompatibility for wound repair

Raniya Razif, Andik Nisa Zahra Zainuddin, Nurul Ain Zawawi, Manira Maarof, Haslina Ahmad, Fatimah Mohd nor & Mh Busra Fauzi

To cite this article: Raniya Razif, Andik Nisa Zahra Zainuddin, Nurul Ain Zawawi, Manira Maarof, Haslina Ahmad, Fatimah Mohd nor & Mh Busra Fauzi (2026) Preliminary genipin-crosslinked gelatin–asiaticoside injectable hydrogel for future biomaterials ink: physicochemical properties and cytocompatibility for wound repair, Artificial Cells, Nanomedicine, and Biotechnology, 54:1, 159-191, DOI: 10.1080/21691401.2026.2627111

To link to this article: https://doi.org/10.1080/21691401.2026.2627111

Published online: 18 Feb 2026.

ARTIFICIAL CELLS, NANOMEDICINE, AND BIOTECHNOLOGY
2026, VOL. 54, NO. 1, 159–191
https://doi.org/10.1080/21691401.2026.2627111

Preliminary genipin-crosslinked gelatin–asiaticoside injectable hydrogel for future biomaterials ink: physicochemical properties and cytocompatibility for wound repair

Raniya Razif[a], Andik Nisa Zahra Zainuddin[a], Nurul Ain Zawawi[a], Manira Maarof[a,b], Haslina Ahmad[c,d], Fatimah Mohd nor[e] and Mh Busra Fauzi[a,b]

[a]Department of Tissue Engineering and Regenerative Medicine (DTERM), Faculty of Medicine, Universiti Kebangsaan Malaysia, Kuala Lumpur, Malaysia; [b]Advance Bioactive Materials-Cells UKM Research Group, Universiti Kebangsaan Malaysia, Bangi, Selangor, Malaysia; [c]Integrated Chemical Biophysics Research, Universiti Putra Malaysia (UPM), Selangor, Malaysia; [d]Department of Chemistry, Faculty of Science, Universiti Putra Malaysia (UPM), Selangor, Malaysia; [e]KPJ Ampang Puteri Specialist Hospital, Ampang, Malaysia

ABSTRACT

Chronic wounds remain a major healthcare concern due to delayed healing and high risk of infection. This study investigates the potential of genipin-crosslinked gelatin and asiaticoside (ASI) as innovative biomaterials ink for wound healing. Hydrogels were prepared using different concentrations of gelatin (9% w/v and 10% w/v) and asiaticoside at 0.05% w/v, with genipin employed as a natural crosslinker to improve mechanical strength. Their physicochemical characteristics, which includes swelling ratio, water vapour transmission rate (WVTR), contact angle, porosity, enzymatic degradation, and surface roughness were systematically evaluated, along with mechanical and cytotoxicity properties. Incorporation of asiaticoside enhanced hydrogel hydrophilicity, reduce porosity, and improved swelling behaviour, while preserving biodegradability and overall structural stability. The WVTR values remained within the optimal wound healing range (1500–2500 g/m^{2}h). Furthermore, asiaticoside-loaded hydrogels demonstrated excellent cytocompatibility, supporting fibroblasts viability at lower concentrations including live/dead assay tests that were conducted. This study demonstrates that genipin-crosslinked gelatin–asiaticoside hydrogels are promising biomaterials ink for accelerated wound healing, with an initial characterization of an injectable formulation guiding their successful optimization to achieve the optimal injectability and printability for tissue engineering and three-dimenstional bioprinting (3D-bioprinting).

GRAPHICAL ABSTRACT

Flow of the study of the Gelatine-ASI biomaterial inks. Images were created using https://BioRender.com (accessed on 21 August 2025).

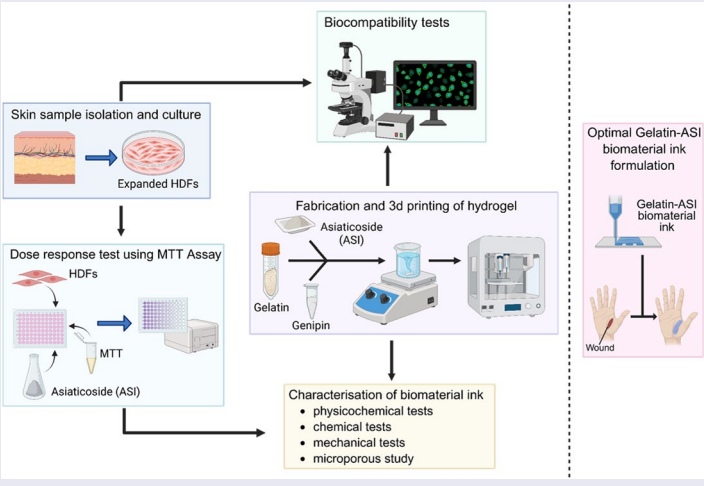

ARTICLE HISTORY

Received 2 October 2025
Revised 28 January 2026
Accepted 2 February 2026

KEYWORDS

Injectable hydrogel; biomaterial inks; 3D-bioprinting; gelatin; asiaticoside; wound healing

CONTACT Mh Busra Fauzi fauzibusra@ukm.edu.my Department of Tissue Engineering and Regenerative Medicine, Faculty of Medicine, Universiti Kebangsaan Malaysia, 56000, Kuala Lumpur, Malaysia.

Introduction

The skin is the body's first line of defence, acting as a protective barrier that shields against microbial invasion and physical trauma, while also regulating temperature, hydration and electrolyte balance [1,2]. Beyond these roles, the skin contributes to physiological homoeostasis through immune and neuroendocrine mechanisms [2,3]. A wound is essentially damage to skin tissue caused by trauma, burns or disease, and it is categorized as either acute or chronic depending on its healing duration. Acute wounds generally resolve in a short time, whereas chronic wounds, often associated with diabetes, obesity or vascular disorders, heal poorly and, if untreated, may pose serious health risks [4]. Diabetes mellitus (DM) is a metabolic disorder that affects almost every country. In 2019, it was predicted that 463 million individuals worldwide were suffering from diabetes, and the number is expected to increase in the following years.

Cutaneous tissue loss, which involves the destruction of skin layers and sometimes deeper structures, is a common consequence of wounds, particularly chronic ones, and can disrupt physiological balance and lead to disability [5,6]. In diabetes, such tissue loss is closely linked to complications arising from poor glycaemic control. Elevated blood glucose can cause microvascular dysfunctions like neuropathy, nephropathy, and retinopathy, all of which compromise skin integrity and delay repair. Additionally, diabetic individuals are more prone to infections such as cutaneous candidiasis. Their impaired immune responses, further aggravate tissue damage and hinder healing. The burden is substantial as cutaneous tissue loss affects roughly 8.5 million individuals in the United States, with an economic impact of USD 28–90 billion annually [7,8]. The condition not only imposes financial strain but also diminishes patients' quality of life, as persistent wounds contribute to physical disability and psychological stress, limiting daily activities and social interactions [9].

Conventional wound care approaches, including grafts, debridement, skin flaps, and non-surgical options like antiseptics and dressings are widely practiced [10,11]. However, their effectiveness is often inadequate for chronic wounds, necessitating adjunctive therapies or specialized treatment programs [12,13]. Advances in tissue engineering provide promising alternatives by using bioactive scaffolds, stem cells, and skin substitutes to accelerate repair and reduce scarring [14]. Recent literature emphasizes a paradigm shift towards functionalized hydrogels that actively remodel the wound microenvironment rather than serving merely as passive coverings. For instance, one study developed responsive multifunctional hydrogels designed to emulate the chronic wound-healing cascade, successfully transitioning wounds from the inflammatory to the proliferative phase [15]. Similarly, injectable hydrogels based on recombinant humanized collagen have been shown to repair damaged tissue by effectively remodelling the local microenvironment and inhibiting apoptosis [16]. These innovations highlight the growing need for biomaterials that offer not only structural support but also active therapeutic intervention to address the complex pathology of chronic wounds. A key innovation in this field is 3D bioprinting, which enables the design of customizable scaffolds composed of injectable hydrogels and biomaterial inks that encourage tissue regeneration and vascularization [17]. These 3D-printed constructs are tailored to mimic the extracellular matrix (ECM), improving integration and healing [18,19]. Biomaterial inks, typically composed of biomaterials, living cells, and bioactive molecules, are deposited in layers to build three-dimensional scaffolds that better replicate the dynamic properties of natural tissues [20–22]. For wound-healing applications, effective biomaterial inks must therefore balance injectability, mechanical stability, degradation behaviour and biologically relevant activity within the selected formulations.

Gelatin, obtained from collagen in sources such as fish, bovine and porcine tissues, is widely used in biomedical applications due to its low immunogenicity, biocompatibility and ease of modification [23]. Gelatin-based hydrogels closely mimic the mechanical environment of soft tissues and support wound repair [24,25]. They are also cost-effective, derived from collagen-rich by-products and offer biodegradability, biocompatibility and non-toxicity. Genipin, a natural crosslinking agent, enhances gelatin hydrogels by improving the overall hydrogels' properties including mechanical strength, thermal stability, enzymatic resistance and swelling capacity, while maintaining low cytotoxicity [26–31]. Asiaticoside (ASI) is a triterpene ester glycoside bioactive compound found in Centella asiatica. It has therapeutic properties that allow for better and faster wound healing especially for chronic wounds that have a high tendency for prolonged healing [32–34]. Asiaticoside exhibits an extensive spectrum of pharmacological properties, including neuroprotective, cardioprotective, hepatoprotective, wound-healing, anti-inflammatory, antioxidant, anti-allergic, antidepressant, anxiolytic, antifibrotic, antibacterial, anti-arthritic, antitumour and immunomodulatory

effects [35]. Importantly, asiaticoside has low toxicity and is capable of wound healing without inducing harmful side effects [36].

While asiaticoside (ASI) is widely recognized for its wound-healing bioactivity, its role in gelatin-based biomaterial inks has predominantly been described as therapeutic additive rather than a functional network modifier. Most gelatin-based hydrogel systems incorporating bioactive compounds primarily aim to enhance cellular responses, with limited consideration of how these molecules influence the physicochemical assembly, gelation behaviour, and microstructural organization of the hydrogel matrix itself [15]. As a result, the potential of asiaticoside to contribute beyond biological stimulation **r**emains underexplored in the context of injectable and printable biomaterials.

Structurally, asiaticoside contains multiple hydroxyl-rich glycosidic moieties that are capable of forming hydrogen-bonding interactions with polymeric chains [34]. These interactions can influence polymer-polymer associations, crosslinking efficiency, and network packing density. In gelatin-based systems, such molecular interactions may alter gelation kinetics, pore architecture, surface roughness, hydrophilicity, and rheological behaviour-properties that are critical for injectability and extrusion fidelity for 3D bioprinting applications. Importantly, these physicochemical effects are distinct from asiaticoside's well-documented biological activity and may confer functional advantages in biomaterial ink design.

Therefore, in this study, asiaticoside is not treated solely as a bioactive agent but as a multifunctional component capable of simultaneously modulating the biological and physicochemical performance of a genipin-crosslinked gelatin hydrogel system. By integrating asiaticoside at a low, cytocompatible concentration, this work seeks to demonstrate a synergistic effect in which gelatin provides a biocompatible scaffold, genipin ensures mechanical stability and controlled degradation, and asiaticoside actively tunes network structure and injectability. This approach distinguishes the present biomaterial ink from conventional gelatin-based biomaterial inks and supports its potential application in wound healing and future 3D bioprinting strategies. By combining gelatin, genipin and asiaticoside, a synergistic biomaterials ink is created that is particularly suitable for tissue engineering purposes. Genipin reinforces scaffold strength and degradation control, while asiaticoside imparts antimicrobial activity and supports cellular proliferation and differentiation. Together, they yield a hydrogel with optimized bioactivity and stability, tailored for regenerative medicine [26,30]. In this work, we developed biomaterial ink comprising gelatin crosslinked with genipin and supplemented with asiaticoside, designed to enhance wound healing. As illustrated in the graphical abstract, this study aimed to develop a candidate for skin tissue repair and 3D bioprinting by first characterizing an injectable formulation to guide optimization, and then evaluating its physicochemical properties and cytotoxicity based on the hypothesis that asiaticoside would enhance bioactivity while genipin would improve mechanical stability.

Study design

The study design was approved by the Universiti Kebangsaan Malaysia Research Ethics Committee (Code no. JEP-2024-904). In contrast to the previously published article on Kelulut honey, the present study investigates a different formulation centred on asiaticoside (ASI), a bioactive compound derived from *Centella asiatica* that is widely recognized for its wound healing properties. While both studies share the same aim of developing viable biomaterials inks for wound healing, the active ingredients, crosslinking strategies, and experimental emphases differ. Both studies were conducted under the same ethical approval granted by the Universiti Kebangsaan Malaysia Research Ethics Committee, which encompasses the collection and use of human dermal fibroblasts and tissue samples for biomaterials-related research. As a result, the same ethical approval number is cited in both publications. The earlier publication primarily addressed the physicochemical characterization of gelatin-Kelulut honey hydrogels, focusing on their gelation, swelling, degradation, and structural stability. In contrast, the current study advances the research by formulating gelatin-genipin hydrogels incorporating asiaticoside and conducting a more comprehensive characteristics evaluation. Specifically, this work includes an assessment of cytocompatibility with primary human dermal fibroblasts and exploration of the potential use of these hydrogels as biomaterials ink in 3D bioprinting applications. These additional biological and translational dimensions extend the scope of the previous study beyond physicochemical characterization, thereby providing new insights into how asiaticoside-based biomaterials can actively promote skin regeneration and wound repair. As for the asiaticoside powder that is being used for this study, it was provided by Barentz Sdn Bhd.

Primary human dermal fibroblasts were isolated from redundant skin tissues obtained from patients undergoing surgery. Written informed consent was obtained from all participants before sample

collection, in accordance with the Declaration of Helsinki and institutional ethical guidelines.

Skin sample isolation and culture

Primary human dermal fibroblasts (HDFs) were isolated from redundant skin tissues collected from five consenting patients undergoing abdominal surgery such as appendicitis and abdominoplasty at Hospital Canselor Tuanku Mukhriz (HCTM), Malaysia. The tissues were surplus material that would otherwise have been discarded, and no additional procedures were performed specifically for this study. Written informed consent was obtained from all participants prior to tissue collection. Inclusion criteria were patients aged 19–60 years undergoing abdominal surgery (appendicitis, abdominoplasty, etc.) without chronic disease (e.g. diabetes). Exclusion criteria were patients with severe infection under antibiotic treatment or tissue fragments smaller than 1 cm^2.

Enzymatic digestion of skin samples was performed using 0.6% w/v collagenase type I (Worthington-Biochemical Corporation, 730 Vassar Ave, Lakewood, NJ, USA) and trypsin-EDTA (Gibco, Carlsbad, CA, USA), with Dulbecco's phosphate-buffered saline (DPBS; Gibco, Carlsbad, CA, USA) washes, followed by centrifugation and resuspension in Dulbecco's modified Eagle's medium/nutrient mixture F12 (DMEM/F12) supplemented with 10% w/v foetal bovine serum (FBS; Gibco/BRL, Carlsbad, CA, USA). Cells were seeded in 6-well plates, cultured until 70-80% confluence, and then subcultured. Expanded HDFs were maintained in flasks containing DMEM/F12 with 10% w/v FBS [37]. The experimental workflow is illustrated in Figure 1.

Dose-response test

The cytotoxicity of asiaticoside (Givaudan SA, Vernier, Geneva, Switzerland) was assessed *via* an MTT (3-[4,5-dimethylthiazol-2-yl] – 2,5-diphenyl tetrazolium bromide) assay. In this procedure, 10,000 cells per well were first cultured for 24 h in 48-well plates. The cells were subsequently exposed to varying concentrations of asiaticoside for 24, 48, or 72 h. Cell viability was then quantified by adding MTT reagent, incubating for 4 h, dissolving the subsequent formazan crystals in DMSO, and reading the absorbance at 540 nm. The number of viable cells is directly proportional to the measured absorbance.

Hydrogel preparation

Two different gelatin (GE) solutions, one at 9% (w/v) and the other at 10% (w/v), were prepared. This was achieved by dissolving GE powder (Nitta-Gelatin Ltd., Japan) in distilled water (dH_2O) at 40 °C with constant stirring (300 rpm) for 30 min, until a homogeneous solution was obtained. Next, ASI powder was incorporated into each gelatin solution to create 9GE_ASI and 10GE_ASI formulations, respectively. Finally, a 0.1% (w/v) Genipin (GNP; FUJIFILM Wako, Japan) solution, prepared in 70% ethanol (EtOH; MERCK, Germany), was added to both formulations as a cross-linker. The fabrication of the hydrogels *via* printing was performed through the extrusion of biomaterial inks. These materials were initially loaded into syringes and then dispensed using a Biogen XI 3D bioprinter (3D GENS; Shah Alam, Selangor, Malaysia) under thermal conditions of 23 ± 2 °C.

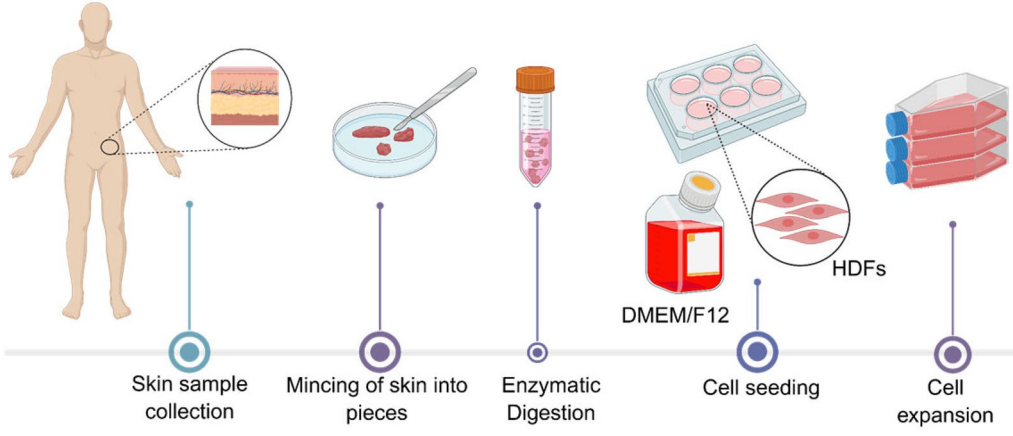

Figure 1. Experimental design for human skin cell isolation. Images were created using https://BioRender.com (accessed on 21 August 2025).

Gelation and injectability

The gelation process of the hydrogels was monitored at a temperature of 23 ± 2 °C, and the time required for complete gelation was recorded using the inverted tube test method.

Evaluation of gross appearance and 3D-bioprinting

The impact of ASI on the extrudability of hydrogels for biomaterial ink applications was evaluated by comparing the gross morphology of ASI-containing formulations to those of the controls (9GE and 10GE). All hydrogels were extruded through a syringe and nozzle, after which their final appearance was reported with a digital camera (Nikon, Tokyo, Japan), capturing both top and lateral images. Also, a 3D bioprinter (BiogensX1) was utilized to print the hydrogel, and the overall gross appearance was assessed. Print fidelity and filament uniformity were quantitatively evaluated from printed constructs using ImageJ software (v1.54k, NIH, USA). The printed filament widths were measured at 10 random locations per construct and compared with the 22 G nozzle with diameter of 0.4 mm. Print fidelity was calculated as the ratio between printed filament width and nozzle diameter. The extrusion pressure applied during printing was not recorded due to instrument limitation, but rheology analysis in this study is sufficient to understand the behaviour of the extrusion pressure of the formulations. Filament uniformity was assessed using the coefficient of variation (CV%), calculated as the standard deviation divided by the mean filament width. This approach has been widely adopted to assess extrusion-based biomaterial ink performance and structural stability [38,39].

Swelling ratio

The swelling behaviour of the hydrogels was investigated to assess their fluid absorption capacity, following a modified procedure from [31]. Freeze-dried samples were weighed for their initial weight (Wi), submerged in DPBS (pH 7.4) at room temperature for 6 h, and then weighed again for their final weight (Wf) after the careful removal of excess buffer. The swelling ratio was then calculated from these weights using the following formula:

$$Swelling\,ratio\left(\%\right)=\frac{\left(Wf-Wi\right)}{Wf}\times 100$$

Porosity

Two different methods, described below, were used to determine and compare the porosity of the freeze-dried hydrogels.

Scanning electron microscopy (SEM)

The microstructure of the hydrogels was visualized using a Supra 55VP field-emission scanning electron microscope (FESEM, Jena, Germany). Before imaging, the hydrogel samples were prepared by freeze-drying followed by the deposition of a thin gold coating to improve image clarity; this procedure followed a previously reported method [40]. The resulting micrographs were then processed with ImageJ software (v1.54k, National Institutes of Health, Bethesda, MD, USA). for the measurement and calculation of the pore diameters.

Liquid displacement

The porosity of the hydrogel scaffolds was quantified using a liquid displacement technique. Ethanol was selected as the displacement medium due to its nature as a non-solvent for the hydrogel's polymeric network [41]. This selection is critical as ethanol does not induce swelling or cause dimensional changes to the scaffold, thereby preserving its native architecture. Instead of interacting with the polymer, the ethanol readily infiltrates the porous matrix, filling the interstitial void spaces, which allows for an accurate determination of the total pore volume. To conduct the measurement, pre-weighed, lyophilized hydrogel samples were fully submerged in ethanol. The percentage porosity was then calculated from the change in mass recorded before and after this immersion, according to the formula presented below:

$$Porosity\left(\%\right)=\frac{Wf-Wi}{pV}\times 100$$

In this expression, the variables Wi and Wf refer to the initial (dry) and final (ethanol-saturated) weights of the hydrogel scaffold, respectively. The other parameters, ρ and V, represent the density of ethanol (0.789 g/cm^3) and the total volume of the scaffold.

Contact angle

The surface hydrophilicity of the polymerized hydrogels was characterized through contact angle analysis. This measurement was performed by placing a 10 µL droplet of distilled water onto the hydrogel surface [42]. The image of the droplet was then captured with

a digital camera, and the contact angle was subsequently calculated from this image through analysis with ImageJ software (v1.54k, National Institutes of Health, Bethesda, MD, USA).

Water vapour transmission rate

The Water Vapour Transmission Rate (WVTR) was measured using an American Society for Testing and Materials (ASTM) standard method [40,43] to assess the hydrogels' suitability for wound healing. Each hydrogel sealed a jar containing 10 ml of distilled water, and they were incubated at 37 °C in 5% CO_2. WVTR was calculated with the following equation, where Wi and Wf are the initial and final assembly weights, and A is the surface area.

$$WVTR = \frac{(Wf - Wi)}{(A \times Time)}$$

Enzymatic degradation

To assess enzymatic degradation, pre-weighed (W1) hydrogels were incubated in 0.0006% (w/v) collagenase type-I (Worthington, Lakewood, NJ, USA) for 6 h at 37 °C. The hydrogels were then rinsed with distilled water, and their final weight (W2) was recorded [44]. The percentage weight loss, indicating biodegradation, was calculated using the following equation:

$$Weight\ Loss(\%) = \frac{(W2 - W1)W1}{W1} \times 100$$

Mechanical testing

Compression and resilience

The mechanical properties of the hydrogels were assessed with a modified compression test [40,43,44]. Cylindrical samples, around 2 cm in diameter and 3 mm in height, were compressed at room temperature. Images of the scaffold were captured before, during, and after compression with a Nikon digital camera. The change in the scaffold's thickness was then measured from these images using ImageJ software (v1.54k, National Institutes of Health, Bethesda, MD, USA). The percentages for compression and resilience were calculated using the formula below.

$$Compression(\%) = \frac{Ac}{Ai} \times 100$$

$$Resilience(\%) = \frac{Af}{Ai} \times 100$$

In the equation, Ai is the initial thickness, Ac is the thickness during compression, and Af is the final recovered thickness of the hydrogel.

Rheology testing

An analysis of the hydrogels' viscoelastic properties was performed at 23 °C on an AR2000 rheometer (TA Instruments). The measurement setup consisted of a 20 mm parallel plate geometry with the gap set to 2000 µm. An oscillating frequency sweep, conducted over an angular frequency range of 0.1 to 100 rad/s, was used to determine the storage modulus (G′), loss modulus (G′′), and complex viscosity (η∗). In a separate experiment, the effect of temperature on the biomaterial inks' viscosity (η) was investigated using a flow temperature-ramp test, which cooled the samples from a starting temperature of 27 °C to a final temperature of 19 °C [44].

Atomic force microscopy (AFM)

The surface roughness of the freeze-dried hydrogels was analysed by Atomic Force Microscopy (AFM; Park Systems NX-10 instrument, Suwon, Korea). Images were acquired in non-contact mode using a 0.2 Hz scan rate, a 5 × 2 nm scan size, and a 256 × 256-pixel resolution. The XE Image Processing Program was then used to quantify surface roughness from the data obtained from the 5 × 5 mm samples.

Sample characterization

Fourier-transform infrared (FTIR)

Fourier-transform infra-red (FTIR) spectroscopy (Perkin Elmer, Waltham, MA, USA) was used to investigate the hydrogels' chemical structure, including changes from crosslinking and the addition of asiaticoside. Spectra were acquired from 4000 cm^{-1} to 500 cm^{-1} to determine characteristic functional groups based on their absorbance peaks.

Energy-dispersive X-ray (EDX)

The elemental composition of the hydrogels was determined by energy-dispersive X-ray (EDX) analysis on a Phenom Pro X SEM EDX microscope. Commercial gelatin, genipin powder, and asiaticoside were used as controls.

X-ray diffraction (XRD)

The crystalline structure of the hydrogel was characterized using X-ray diffraction. This analysis was performed with a D8 Advance X-ray diffractometer

(Bruker, Coventry, UK), which was operated under a temperature control spanning from 0 to 80 °C. The resulting diffraction patterns, plotted as a function of the diffraction angle 2θ, were subsequently processed and analysed using the accompanying Diffrac [45]. Suite EVA software package (V4.0, Bruker, Coventry, UK).

Cytotoxicity evaluation on hydrogel scaffolds

Hydrogel biocompatibility with human dermal fibroblasts (HDFs) was assessed using the LIVE/DEAD™ Cytotoxicity Kit (Thermo Fisher Scientific, Waltham, MA, USA). To prepare the samples, hydrogels were produced aseptically. The biomaterial components were UV-sterilized, while the distilled water was autoclaved. The sterile hydrogels were then polymerized in 48-well plates, seeded with HDFs (3.5×10^4 cells), and cultured for 24 h [30]. For analysis, the samples were incubated for 30 min at 37 °C with a solution of 2 mM calcein-AM and 4 mM ethidium homodimer-1 (EthD-1). Cytotoxicity was subsequently analysed *via* fluorescence microscopy (Nikon A1R-A1, Tokyo, Japan) at 100× magnification. Due to restrictions in the current ethical approval, which does not permit blood collection from human samples, hemocompatibility testing, which is haemolysis ratio assay was not conducted in this study.

Scratch assay

The *in vitro* wound-healing potential of the developed hydrogel formulations was evaluated using a scratch wound-healing assay, which assesses collective cell migration of human dermal fibroblasts (HDFs). This assay was employed to compare the effects of formulated hydrogels on fibroblast migration, which is a critical process in wound closure and tissue regeneration. HDFs were seeded into 12-well plates at a density of 2.0×10^5 cells per well and cultured in complete DMEM/F12 supplemented with 10% (w/v) fetal bovine serum until 70–80% confluence was achieved (18–24 h). A linear scratch was created across the cell monolayer using a sterile 1 ml pipette tip held perpendicular to the well surface. Detached cells were removed by gentle washing with DPBS, followed by replacement with fresh culture medium. Phase-contrast images of the scratch area were captured immediately after scratching which is 0 h and at subsequent time points up to 24–48 h. Wound closure was quantified by measuring the reduction in scratch area over time using ImageJ software. The percentage of wound closure was calculated using the following formula [45].

$$\text{Wound closure}\,(\%) = \frac{A_0 - A_t}{A_0} \times 100$$

Statistical analysis

All data were processed and analysed using GraphPad Prism software (V10.0, GraphPad Software Inc., San Diego, CA, USA). Throughout this manuscript, *N* refers to the number of independent experimental units, which are biological replicates for cell studies and independent fabrication batches for physicochemical studies. While *n* refers to the number of technical replicates, which are repeated measurements within the same independent unit. To ensure statistical rigour, technical replicates, *n* were averaged to generate a single mean for each independent unit *N* prior to analysis. Statistical significance was calculated using the means of independent units *N*, not technical replicates, to avoid pseudoreplication. The experimental results, which were gathered from three independent replicates ($N = 3$), are expressed as the mean ± standard deviation. To determine significant differences among multiple groups, one-way and two-way analysis of variance (ANOVA) were performed. A p-value of less than 0.05 was established as the standard for statistical significance with exact p-value also being mentioned for more in depth statistical analysis. Effect sizes were also calculated as eta squared (η^2) for one-way ANOVA and partial eta squared (ηp^2) for two-way ANOVA. As for effect size, value above 0.14 is considered as large effect size with the factors having significant effect on the outcome [46].

Results

Dose–response test with asiaticoside

Figure 2 shows the dose-dependent effect of ASI on human dermal fibroblast (HDFs) viability ranging from 0.01% w/v, 0.05% w/v, 0.1% w/v, 0.5% w/v to 1.0% w/v and across 24, 48, and 72 h timepoints. Cell viability of HDFs remained relatively high at lower concentrations of asiaticoside ranges from 0.01% w/v to 0.1% w/v at 24 h and 48 h' time points with 0.01% w/v having above 100% cell viability for both time points. Over 72 h, gradual decline can be seen for 0.05% w/v and 0.1% w/v while still being minimal reduction and within good cell viability range. This shows that at lower concentrations, asiaticoside has potential to promote cell proliferation or low to non-cytotoxic effect on HDFs. In comparison, a significant drop in cell viability can be seen at 0.5% w/v especially at 48 h, and

72 h' time points reaching close to 0% viability which indicate cytotoxic threshold. A strong cytotoxic effect was also observed at 1.0% w/v concentration as the cell viability dropped tremendously across all time points being below 50% and reaching 0% cell viability, confirming the detrimental effect of high concentrations of asiaticoside towards HDFs. The cell viability dropped at the highest concentration of 1.0% w/v for 24 h and 72 h are significant reduction compared to 0.01% w/v, 0.05% w/v, and 0.1% w/v at 24 h' time point as can be seen by the significant difference marker (****, $p < 0.0001$) and the severity dropped in percentage of viable cells. This significant dose-dependent cytotoxicity shows that asiaticoside has a critical threshold that must be followed to maintain the beneficial effects and be harmless to HDFs' viability. In addition, a trend of reduction in cell viability across all concentrations can be seen for longer incubation time, especially for higher concentrations indicating the cumulative of cytotoxic effects of asiaticoside towards HDFs after very long exposure. A significant main effect of ASI concentration on HDF viability $\eta p^2 = 0.77$, was demonstrated indicating a large effect size, as well as a significant effect of exposure time $\eta p^2 = 0.32$. The effect size indicates that both ASI concentration and exposure time have significant effect on HDFs viability these factors exert a strong and meaningful influence on HDFs viability.

The selection of 0.05% w/v asiaticoside (ASI) for hydrogel fabrication was informed by a dual optimization strategy involving both biological safety and physicochemical functionality. *In vitro* studies have consistently established that asiaticoside enhances key wound healing processes, including dermal fibroblast proliferation, migration, and adhesion, specifically at non-toxic concentrations. For instance, previous research has demonstrated that ASI promotes the migration and growth of normal human skin cells with no cytotoxic effects within a specific low-dose range, while also upregulating extracellular matrix synthesis, particularly type I and III collagen expression [47,48].

Conversely, higher concentrations tend to exert adverse effects on cellular viability. This aligns with general pharmacological observations that phytoconstituents operate within a narrow therapeutic window, beyond which cellular stress responses predominate. Our dose-dependent cytotoxicity results confirmed this in Figure 2. While 0.1% w/v appeared viable initially, a gradual decline was observed after 72 h, indicating potential cumulative stress.

Furthermore, from biomaterials design perspective, preliminary screening indicated that the lowest concentration (0.01% w/v) was insufficient to significantly modulate the hydrogel's bulk properties. As shown in Figure 3(a), a loading of 0.05% w/v was required to effectively accelerate gelation kinetics and enhance hydrophilicity. Consequently, 0.05% w/v was selected as the optimal formulation as it represents the highest cytocompatible dose that ensures beneficial cellular responses while providing sufficient bioactive loading to modulate hydrogel physicochemical properties without deleterious effects on fibroblast viability suitable for wound-healing applications.

Gross appearance and gelation time

Figure 3(a) shows how different biomaterial ink formulations affect gelation time. Generally, higher polymer concentrations are associated with faster gelation, although the addition of asiaticoside alters

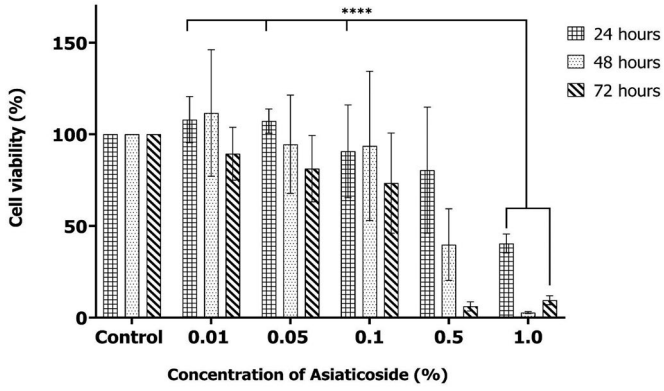

Figure 2. Cytotoxicity of different concentrations of Asiaticoside (0.01%, 0.05%, 0.1%, 0.5%, and 1.0%) (w/v) towards human dermal fibroblasts measured using the MTT assay. Control represents the control media used in the MTT assay. Data represents mean ± SD of $N = 3$ independent biological replicates, with $n = 5$ technical replicates per condition. As for effect size, significant main effect of Asiaticoside concentration where large effect size $\eta p^2 = 0.77$ on cell viability and a significant effect of the exposure time where large effect size $\eta p^2 = 0.32$ was found. **** Indicates $p < 0.0001$.

this relationship. Interestingly, a low asiaticoside concentration (0.01 % w/v) has little to no effect on the gelation time of either the 9GE or 10GE formulations, whereas 0.05 % w/v and 0.1 % w/v concentrations accelerate gelation time in both. For example, the 9GE and 9GE_0.01ASI samples gelate at nearly the same rate, but 9GE_0.05ASI and 9GE_0.1ASI reach complete gelation significantly faster than the unmodified 9GE as can be seen with the significant difference marker (***, $p < 0.001$). The same thing could be said for 10GE formulations except 10GE_0.05ASI that had a tiny bit slower gelation compared to 10GE_0.01ASI and 10GE_0.1ASI. Moderate main effect of formulations concentration on gelation time with moderate effect size where $\eta p^2 = 0.12$, alongside a significant main effect of asiaticoside presence with a large effect size where $\eta p^2 = 0.42$ were also found from statistical analysis. These results indicate that asiaticoside concentration plays a critical role in tuning gelation kinetics, potentially

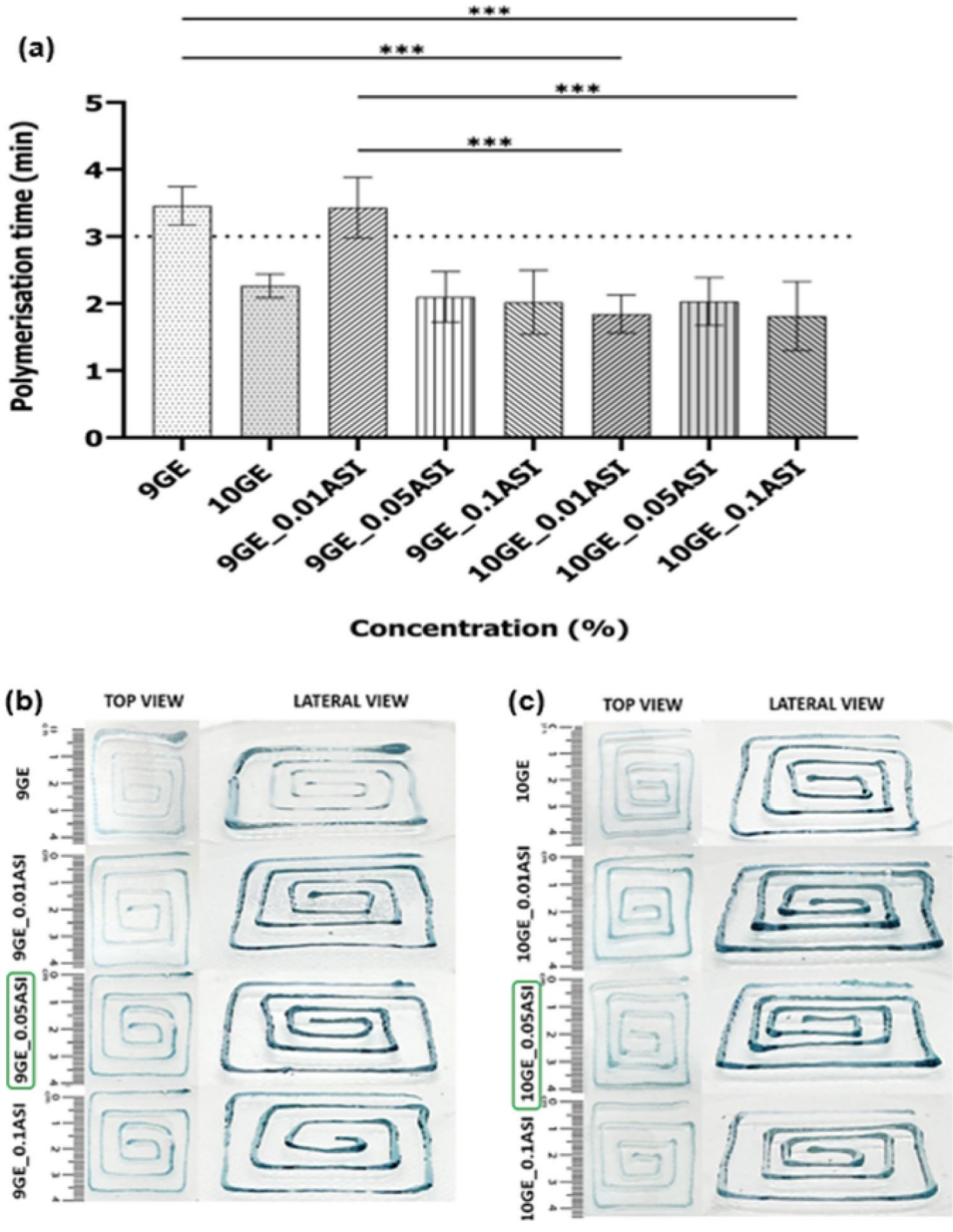

Figure 3. **(a)** The gelation times for 9GE and 10GE hydrogels with and without Asiaticoside (*** indicates $p < 0.001$, where $p = 0.0002$), **(b)** Gross appearance with top and side view of 9GE and **(c)** 10GE hydrogels with and without Asiaticoside. Data represents mean ± SD of $N = 3$ independent fabrication batches, with $n = 5$ technical replicates per condition. Gross appearance images are best representative of $N = 3$ independent fabrication batches. A moderate effect size where $\eta p^2 = 0.12$ was found for the effect of concentrations of formulations on polymerization, while significant main effect of ASI presence on polymerization time was also observed exhibiting a large effect size $\eta p^2 = 0.42$.

outweighing the effect of polymer concentration alone and offering a simple means to tailor handling time for different biomedical applications.

Figure 3(b,c) illustrates the injectability of each ink formulation, shown from both top and side perspectives. All inks display a light blue to teal colouration and possess a gel-like, viscous consistency, as demonstrated by their ability to retain a coiled shape. They also appear translucent to semi-transparent, with certain formulations exhibiting noticeably greater strand thickness than others.

Physical properties analysis

Swelling ratio, contact angle, water vapour transmission rate (WVTR), and biodegradation rate of the gelatin-ASI hydrogels were measured to assess the physical properties of the hydrogels. The results of the detailed assessment were quantified in Figure 4 showcasing the detailed quantitative data for both ASI-incorporated hydrogels and non-ASI-incorporated hydrogels counterparts.

Hydrogel with high water absorption ability would allow for effective absorption of wound exudate. As

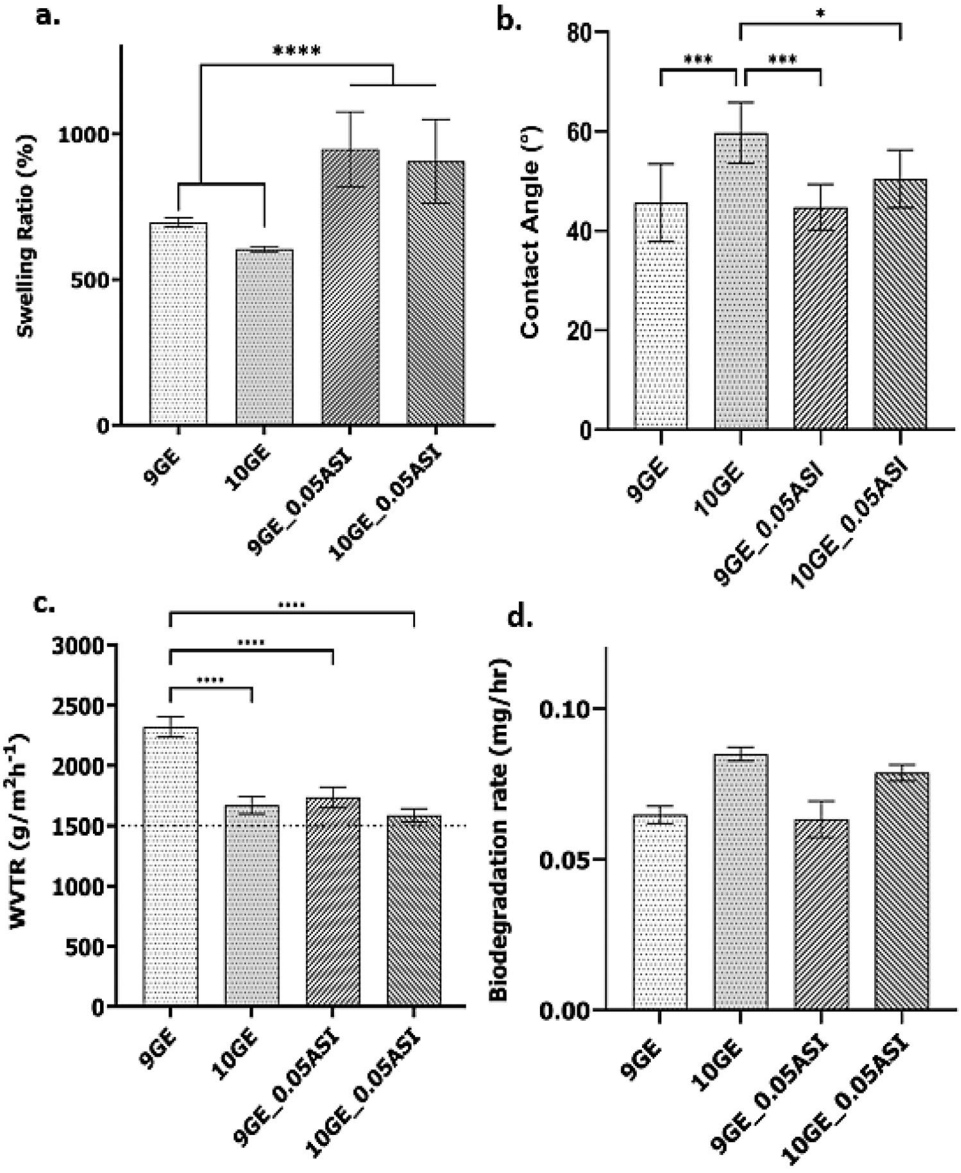

Figure 4. Physical analysis of 9GE, 10GE, 9GE_0.05ASI and 10GE_0.05ASI. (**a**) percentage of swelling ratio, (**b**) contact angle (°), (**c**) Water vapour transmission rate (WVTR) (g/m^2h^{-1}), and (**d**) biodegradation rate. * Indicates $p < 0.05$ where $p = 0.0324$. *** indicates $p < 0.001$ where $p = 0.00021$, and **** indicates $p < 0.0001$ for all graphs. Data represents mean ± SD of $N = 3$ independent fabrication batches, with $n = 5$ technical replicates per condition. As for effect sizes of swelling ratio, contact angle, WVTR, and biodegradation rate are ηp^2 = 0.43, 0.33, 0.67, and 0.15 respectively.

shown in Figure 4(a), all hydrogel formulations showed swelling properties being well above 500%. 9GE_0.05ASI formulation noted the highest swelling capacity of 954.8 ± 96.3%, followed closely by 10GE_0.05ASI formulation with 901.5 ± 89.7% swelling capacity. In addition, high significant differences can be observed through statistical analysis on the swelling behaviour of all the hydrogel formulations. Comparing 9GE and 10GE formulations with their ASI-incorporated formulations, high significant differences were observed through the statistically significant marker (****, $p < 0.0001$) indicating addition of 0.05% w/v of ASI significantly improved water absorption of the formulations through the significantly higher swelling ratio. Thus, incorporation of ASI improves the swelling behaviour of the gelatin-based hydrogel formulations.

Contact angle for gelatin and gelatin-ASI hydrogel formulations can be observed in Figure 4(b). Both ASI-incorporated and non-ASI-incorporated formulations exhibited contact angle below 90°, which indicates hydrophilicity capability. 10GE hydrogel formulations noted the highest contact of 60° ± 11.66°. Addition of ASI into the formulation of 10GE lowered the contact angle for 10GE_0.05ASI (52.3° ± 8.9°) formulation significantly as can be seen with the statistically significant marker (*, $p < 0.05$) suggesting addition of ASI enhances the hydrophilicity of the 10GE formulation. Furthermore, a comparison between 9GE and 10GE revealed a significant difference, with the 10GE formulation exhibiting a more hydrophobic nature, as the contact angle increased significantly, as can be seen with the *** ($p < 0.001$) statistical significance marker. The contact angle of 10GE was significantly higher than 9GE_0.05ASI and can be seen by the high significance difference *** ($p < 0.001$) statistical significance marker, demonstrating that the addition of 0.05% w/v ASI markedly enhanced hydrophilicity by reducing the contact angle. These observations collectively indicate that while a higher gelatin concentration increases hydrophobicity, ASI incorporation counteracts this effect by enhancing hydrophilicity. The strong statistical significance of these differences underscores the effectiveness of ASI in modifying the hydrogel's wettability.

The water vapour transmission rate (WVTR) results are presented in Figure 4(c), illustrating the relationship between gelatin concentration, ASI incorporation, and water vapour permeability across different hydrogel formulations. Comparison between different biomaterial formulations reveals that 9GE formulation has the highest WVTR value which is $2356.70 \pm 182.40\ g/m^2h^{-1}$ as can be seen in the graph in Figure 4(c). This value significantly surpasses the WVTR of 10GE formulation which is at $1689.20 \pm 210.50\ g/m^2h^{-1}$ and being indicated by the **** ($p < 0.0001$) statistical significance marker. This lower WVTR value of 10GE suggests that higher concentration of gelatin would reduce the water vapour permeability caused by denser gelatin networks. The addition of ASI at a concentration of 0.05% w/v into both 9GE and 10GE formulations results in WVTR values that are lower than 9GE but remain comparable to or slightly higher than 10GE. Specifically, the 9GE_0.05ASI, and 10GE_0.05ASI formulations show highly significant reduction in WVTR compared to 9GE, with the **** ($p < 0.0001$) statistical significance marker indicating that ASI incorporation decreases water vapour transmission. In contrast, the 10GE_0.05ASI formulation also showed a slightly reduced WVTR ($1625.80 \pm 180.70\ g/m^2h^{-1}$) compared to 10GE but without a statistically significant difference. This suggests that while ASI reduces WVTR in both hydrogel formulations, the effect is more pronounced in the 9GE group. These results indicate that the presence of ASI slightly restricts water vapour diffusion, possibly by modifying the internal network structure of the formulation. It is worth noting that all ASI-incorporated hydrogels fall within the acceptable WVTR range of more than $1500\ g/m^2h^{-1}$, highlighting their potential for wound-healing applications requiring controlled moisture balance to prevent desiccation and excessive accumulation of wound exudate.

Figure 4(d) shows the biodegradation rates of gelatin and gelatin–ASI hydrogel formulations. Both non-ASI-incorporated hydrogels exhibited relatively low degradation rates of 0.072 ± 0.015 mg/h and 0.089 ± 0.008 mg/h, respectively. The addition of 0.05% w/v ASI slightly reduced the degradation rate in both formulations. However, this reduction remained comparable to the 9GE and 10GE formulations, as indicated by the absence of statistically significant differences among all groups. These findings suggest that the effect of ASI on the biodegradation rate of the formulations is minimal yet noticeable in reducing the degradation rate of the non-ASI-incorporated hydrogel. Nevertheless, all hydrogel formulations including those with ASI, maintained a biodegradation rate below 0.1 mg/h, confirming that the hydrogels degrade in a controlled manner suitable for sustained support during the wound healing process. The effect sizes for swelling ratio, contact angle, water vapour transmission rate (WVTR), and biodegradation rate were all above 0.14, indicating a large effect and suggesting that both ASI concentration and hydrogel formulation significantly influenced these properties.

Mechanical strength and rheology characterization of the fabricated hydrogels

Compression analysis was conducted on the fabricated hydrogels to test the mechanical strength of the hydrogels because it is a key factor for successful implantation as can be seen in Figure 5(a). There were no significant differences found in terms of compressive strength between the scaffold groups. High compressive strength was demonstrated across all scaffolds as all groups showed ability to support approximately 80% of a 300 g weight including asiaticoside loaded hydrogels.

Figure 5(b) shows the resilience analysis that was conducted on the fabricated hydrogels to assess the capacity of the hydrogel groups to regain their initial conformation following compressive deformation. Based on statistical analysis, there were no significant differences between the groups in terms of resilience as all groups displayed complete shape recovery and high resilience. Overall, a significant effect was measured on the effect of ASI concentrations on the compression and resilience of the hydrogels where ηp^2 = 0.25. This suggests that ASI concentrations do affect the ability of the hydrogel to sustain its shape and size when compressed under weight and being able to return to most of its shape after compressed.

Figure 5(c,d,e) shows the rheology test that was conducted on 9GE and 9GE_0.05ASI formulations assessing complex viscosity, storage modulus, and loss modulus properties. These properties allow for better understanding of the viscous and elastic behaviour of the network of both formulations. Both the 9GE and the 0.05% w/v asiaticoside-loaded variant (9GE_0.05ASI) demonstrate classic shear-thinning behaviour in Figure 5(e). As the oscillatory frequency increases from 0.1 to 100 rad/s, their complex viscosities drop dramatically facilitating ease of injection under high shear. At the lowest measured frequency (0.1 rad/s), 9GE has a η* of approximately 1.2 × 10^7 mPa·s, whereas 9GE_0.05ASI measures about 7.5 × 10^6 mPa·s and slowly dropping to zero as it reaches above 1 angular frequency rad/s. Across the entire sweep, the ASI-containing gel remains consistently less viscous than the control, suggesting that ASI disrupts the gelatin-genipin crosslink network or acts as a plasticizing agent, thereby lowering the resistance to flow. The storage modulus (G′) curves in Figure 5(d) confirm that both hydrogels behave predominantly like soft solids (G′ > G″) across the entire

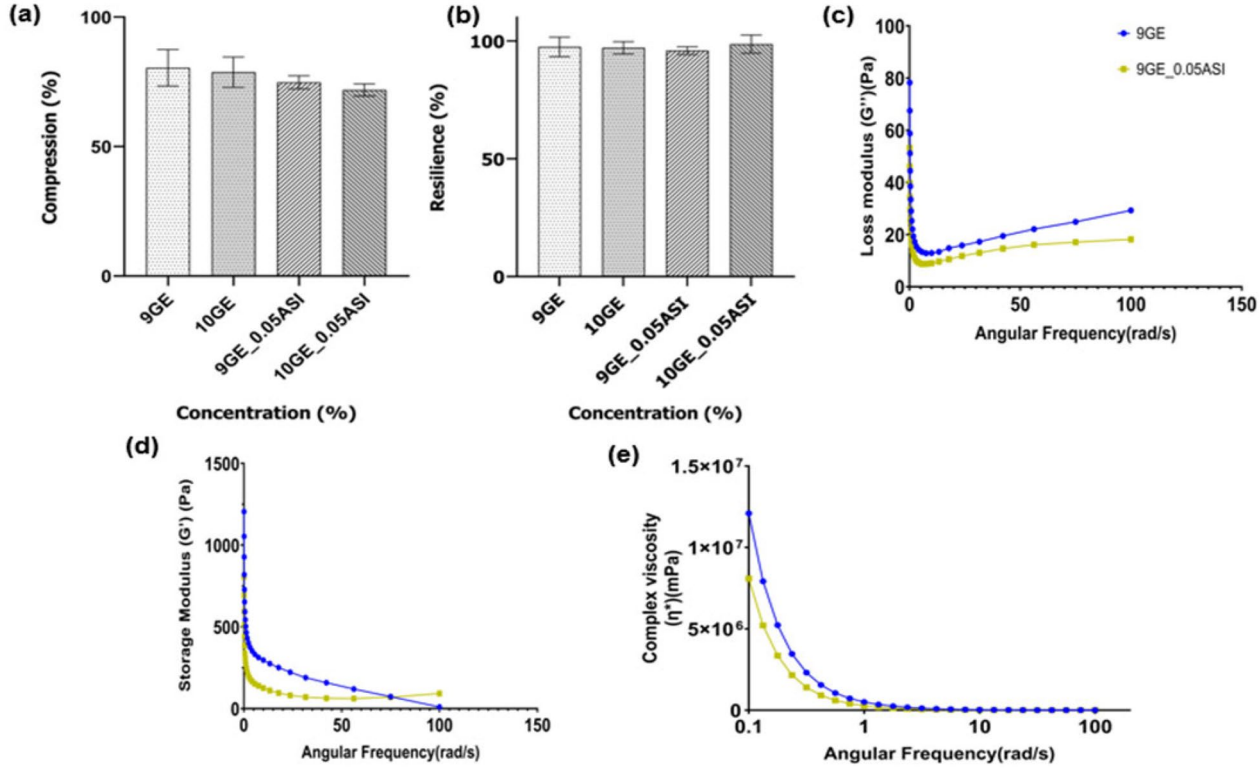

Figure 5. Analysis of the mechanical properties of 9GE, 10GE, 9GE_0.05ASI and 10GE_0.05ASI: (**a**) compression percentage and (**b**) percentage of resilience; analysis of rheology on 9GE and 9GE_0.05ASI: (c) loss modulus, (d) storage modulus and (e) complex viscosity. Data in this figure represents mean ± SD of $N = 3$ independent fabrication batches, with $n = 5$ technical replicates per condition. A large effect size of ηp^2 = 0.25 was found for the effect of Asiaticoside concentrations on the compression and resilience of the hydrogel.

frequency range. At the lowest frequency (0.1 rad/s), 9GE presents a high G′ of ≈1,200 Pa, whereas the ASI-loaded hydrogel is mechanically softer with G′ ≈700 Pa. As frequency increases, G′ for both samples decay steeply, eventually plateauing around 0–50 Pa beyond 50 rad/s. The more pronounced drop in the 9GE_0.05ASI curve indicates that ASI reduces either the density or the strength of elastic crosslinks, which may improve conformability in complex wound geometries. Figure 5(c) shows the loss modulus (G″), a measure of viscous dissipation. Both hydrogels start with G″ values around 80 Pa (9GE) and 60 Pa (9GE_0.05ASI) at 0.1 rad/s, dip to a minimum near 10 Pa at ~10 rad/s, and then gently rise to about 30 Pa by 100 rad/s. Across all frequencies, G″ for the ASI-loaded gel remains lower than that of the control, indicating less energy loss as heat. This further supports the notion of a slightly looser network structure in the presence of ASI.

Chemical characterization of formulations

Figures 6(a) shows FTIR spectroscopy of the fabricated gelatin-based hydrogels which reveal the characteristics of the amine and amide group including hydroxyl group to confirm the structural composition of the scaffolds. This analysis helps to assess and identify the existence of polymers, crosslinkers, including the chemical bonds between the materials used in this study.

In the 3,300 cm^{-1} region ("Amine A"), the broad N–H stretch of gelatin at ~3280 cm^{-1} shifts to ~3260 cm^{-1} in the hydrogels, indicating new hydrogen bonding between gelatin amines and genipin's reactive groups. Genipin itself shows a weaker band here from its secondary amine and hydroxyl groups. Below 3,000 cm^{-1} ("Amine B"), the CH stretching peaks of both gelatin and genipin (2940-2880 cm^{-1}) decrease in intensity and sharpen upon crosslinking, reflecting a more rigid polymer network with reduced segmental motion. The ASI-loaded hydrogels exhibit only subtle alterations in CH band shape, consistent with physical entrapment of asiaticoside rather than covalent modification.

The amide I band of pristine gelatin at ~1645 cm^{-1}, originating from C=O stretching shifts downward to ~1630 cm^{-1} and broadens in the 9GE and 10GE hydrogels. This shift confirms formation of Schiff-base (C=N) linkages between gelatin and genipin and an increase in hydrogen-bonding interactions. Similarly, the amide II band moves from ~1548 cm^{-1} in gelatin to ~1535 cm^{-1} in the crosslinked gels, evidencing altered N-H bending and C-N stretching. In the ASI-containing samples, a minor shoulder near 1520 cm^{-1} suggests overlapping vibrational contributions from asiaticoside's glycosidic or carboxylate groups. The amide III peak of gelatin at ~1240 cm^{-1}, associated with C–N stretching and N–H bending, persists but is slightly attenuated in all hydrogels. Crucially, new weak absorptions appear in the ASI-loaded formulations between ~1030 and 1080 cm^{-1}, characteristic of C-O stretching in asiaticoside's sugar moieties. Additional broad features below 1,000 cm^{-1} further validate the presence of triterpenoid fingerprint vibrations, confirming that asiaticoside is physically entrapped and hydrogen-bonded within the network.

Figure 6(b) displays the X-ray diffraction (XRD) analysis that was conducted for 9GE, 10GE and the ASI-incorporated counterparts which were carried out to analyse the crystallinity and amorphous characteristics of the formulations. All formulations displayed broad

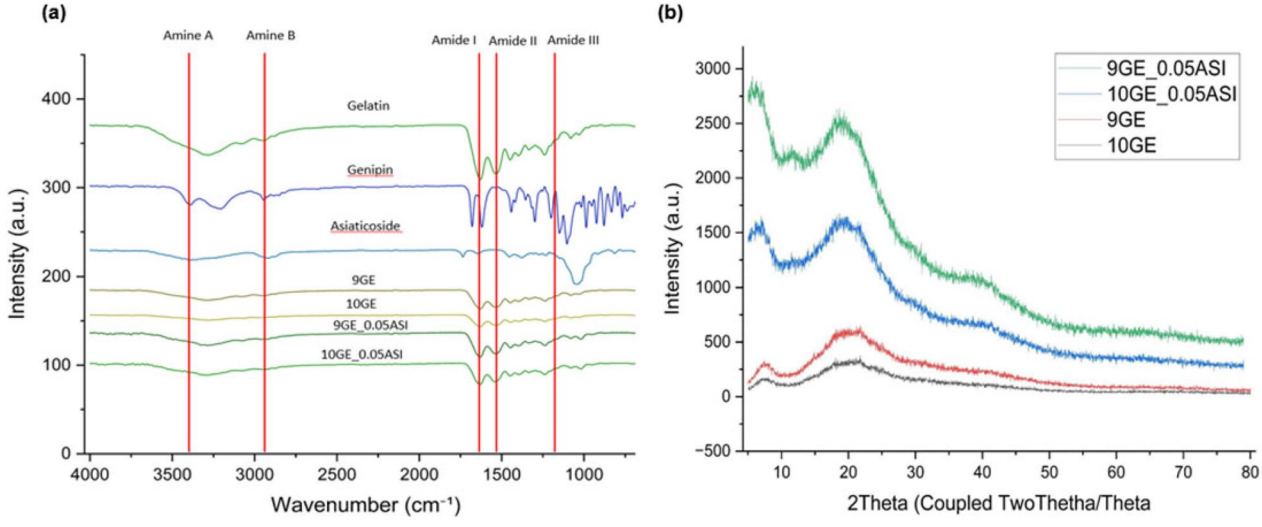

Figure 6. Chemical characterization of the hydrogels and compounds: (a) FTIR spectra and (b) XRD analysis. Data for this figure represent best sample sent to iCRIM Lab in UKM, Malaysia for both analysis of FTIR and XRD.

peaks around 2θ≈20°, characteristic of semi-crystalline or predominantly amorphous polymeric materials. The presence of these broad peaks suggests that the hydrogels predominantly possess amorphous structures with some crystalline domains influenced by crosslinking and additive interactions. Among the samples, 9GE_0.05ASI exhibited the highest peak intensity, followed by 10GE_0.05ASI, 9GE, and 10GE, indicating differences in structural organization across the formulations.

The crystallinity analysis in Table 1 showed that 9GE_0.05ASI recorded the highest crystallinity percentage at 48.13%, suggesting that the addition of ASI at this concentration enhanced the molecular ordering within the hydrogel matrix. This could be attributed to favourable interactions such as hydrogen bonding between gelatin chains and ASI molecules. Interestingly, the addition of ASI in the 10GE_0.05ASI sample resulted in a reduced crystallinity (37.90%), even lower than the control 10GE (41.40%). This suggests that at higher gelatin content, the polymer chains may become overly entangled or sterically hindered, preventing effective integration of ASI and thereby disrupting crystalline domain formation.

In terms of amorphous content, which is inversely related to crystallinity, the 10GE_0.05ASI sample exhibited the highest amorphous percentage (62.10%), followed by 10GE (58.60%), 9GE (53.32%), and 9GE_0.05ASI (51.88%). These results suggest that asiaticoside incorporation tends to increase the amorphous character of hydrogels at higher gelatin concentrations but contributes to a more ordered structure at lower gelatin content. Overall, the 9GE_0.05ASI formulation appears to achieve the most balanced structural properties, combining relatively high crystallinity with manageable amorphous content, which may support both mechanical integrity and functional performance in biomedical applications such as wound healing.

The trend observed also highlights the impact of gelatin concentration on the overall structural arrangement of the hydrogels. An increase from 9% w/v to 10% w/v gelatin resulted in a reduction of crystallinity, which can be explained by the increased density of the crosslinked network limiting the mobility and alignment of polymer chains required for crystalline region development. Correspondingly, the amorphous content increased as crystallinity decreased, with 10GE_0.05ASI showing the highest amorphous percentage at 62.10%. Higher amorphous content typically implies greater flexibility and moisture retention capabilities, which are beneficial features for wound healing materials.

Table 1. XRD analysis for crystallinity and amorphous of hydrogels.

Hydrogels	Crystallinity (%)	Amorphous (%)
9GE_0.05ASI	48.125	51.875
10GE_0.05ASI	37.899	62.101
9GE	46.676	53.324
10GE	41.397	58.603

3D-Microporous structure hydrogel

Figure 7(a) displays the SEM micrographs of 9GE and 10GE and the ASI-loaded counterparts, revealing distinctly heterogeneous porous architectures. The plain 9GE and 10GE samples feature relatively large, well-formed pores with thick walls, giving a more compact appearance. By contrast, loading with ASI produces a much finer, irregular pore network. As can be observed, 9GE_0.05ASI exhibits numerous small cavities and slender struts, while 10GE_0.05ASI shows a similar trend but with pores that are slightly larger and walls that remain comparatively robust. All micrographs were processed in ImageJ (v1.54k, National Institutes of Health, Bethesda, MD, USA) following freeze-drying to ensure consistent pore visualization.

Quantitative analysis confirms these observations as shown in Figure 7(c,b), and Figure 7(d,c). In the 9GE and 9GE_0.05ASI formulations, the average pore size decreased significantly from 221 ± 75 µm to 67 ± 18 µm respectively with the significant difference marker of ** ($p < 0.01$). In the 10GE and 10GE_0.05ASI groups, pores shrank from 181 ± 80 µm to 129 ± 50 µm respectively. Although this reduction is less pronounced than in the 9% (w/v) gelatin formulations, it still demonstrates that ASI incorporation reduces average pore size. The dropped in average pore size between 10GE and 9GE_0.05ASI was also significant showed by the significant difference marker (*, $p < 0.05$). Significant effect of hydrogel formulations and ASI concentrations were also found for both average pore size and Ra value graph indicating both factors having major effects where ηp^2 values are all above 0.14 [46]. These data demonstrate that ASI incorporation induces significant pore refinement and reduced void volume in which the effects are most pronounced at lower gelatin concentrations which potentially enhance scaffold mechanical stability while providing a finely tuned architecture for cell infiltration and controlled bioactive release in wound healing applications.

Table 2 is showing the elemental composition analysis that was conducted on the all formulations through EDX to further understand the chemical properties of the hydrogels.

Both gelatins only groups (9GE and 10GE) exhibited comparable levels of carbon (56.07 ± 0.23% and 56.70 ± 1.07%), oxygen (28.7 ± 1.11% and 28.2 ± 1.90%), and nitrogen (15.2 ± 0.86% and 15.1 ± 1.72%). Introducing 0.05% asiaticoside to 9GE (9GE_0.05ASI) resulted in a reduction of carbon content (53.45 ± 0.49%), along with slight increases in oxygen (28.30 ± 0.71%) and nitrogen

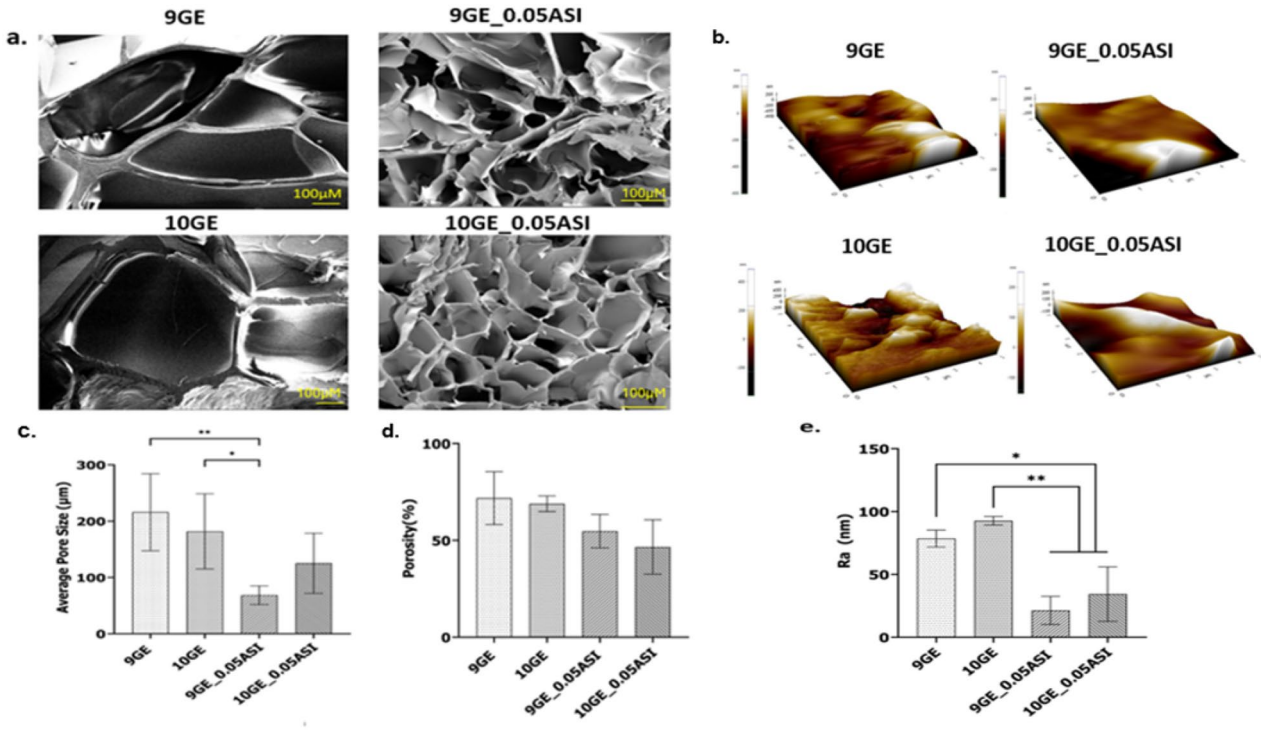

Figure 7. (a) SEM images showing the cross-sectional microporous structure of all hydrogels at 100× magnification; (b) AFM surface topography images; quantitative analysis of (c) average pore size (μm), (d) porosity (%), and (e) surface roughness Ra value. Data are presented as mean ± SD from $N = 3$ independent fabrication batches, with $n = 5$ technical replicates per condition for quantitative measurements. Best representative SEM and AFM images are selected from the independent batches. * Indicates $p < 0.05$ where $p = 0.0233$ for average pore size graph and $p = 0.0340$ for Ra value graph. ** indicates $p < 0.01$ where $p = 0.0079$ for average pore size graph and $p = 0.0088$ for Ra value graph. For average pore size, significant effects were observed for hydrogel formulation where $\eta p^2 = 0.714$ and ASI concentration $\eta p^2 = 0.843$. As for Ra value, main significant effect was observed for hydrogel formulation where $\eta p^2 = 0.628$ and ASI concentrations where $\eta p^2 = 0.733$.

Table 2. Elemental analysis of hydrogels elemental compositions with EDX.

Sample	C (%)	O (%)	N (%)
9GE	56.07 ± 0.23	28.7 ± 1.11	15.2 ± 0.86
10GE	56.7 ± 1.07	28.2 ± 1.90	15.1 ± 1.72
9GE_0.05ASI	53.45 ± 0.49	28.30 ± 0.71	16.00 ± 0.14
10GE_0.05ASI	51.55 ± 1.77	30.15 ± 0.21	16.70 ± 1.56

(16.00 ± 0.14%) levels. A similar pattern was evident in 10GE_0.05ASI, where carbon content dropped further (51.55 ± 1.77%), while oxygen (30.15 ± 0.21%) and nitrogen (16.70 ± 1.56%) contents rose. These shifts in elemental composition suggest that asiaticoside was effectively incorporated into the hydrogel matrix, likely due to its oxygen-rich glycosidic structure and its interaction with gelatin's amino groups.

AFM scanning was conducted on the hydrogel samples and the surface topology of the images can be observed in Figure 7 throughout Figure 7(b,e). Mean surface roughness analysis was also conducted and shown in the graph in Figure 7(e). The surface topography of these hydrogels can significantly influence cell attachment and behaviour. As seen in Figure 7(b) (9GE and 10GE), the samples without asiaticoside exhibit a rougher surface profile, characterized by pronounced peaks and valleys and greater height variations, indicating a higher degree of roughness with 10GE having the roughest surface topology and average surface roughness. In comparison, samples with asiaticoside addition (9GE_0.05ASI and 10GE_0.05ASI in Figure 7(b) appear visibly smoother with more uniform surface features.

Quantitative analysis of average surface roughness (Ra) values confirms these observations, with 10GE showing the highest average roughness, followed by 9GE as can be seen in Figure 7(e). Both asiaticoside-loaded samples displayed significantly reduced Ra values, suggesting a smoothing effect. Statistical analysis revealed a highly significant difference (**$p < 0.01$) between 10GE, 9GE_0.05ASI, and 10GE_0.05ASI, and a moderate significance (*$p < 0.05$) in comparison of 9GE with both ASI-loaded groups, confirming that asiaticoside incorporation effectively reduces surface roughness. Overall, increasing the gelatin concentration tends to raise surface roughness, whereas asiaticoside addition helps create a smoother and more uniform hydrogel

surface, which could potentially improve cellular responses and reduce bacterial adhesion.

Cytotoxicity evaluation and three-dimensional bioprinting on hydrogel scaffold

9GE and 9GE_0.05ASI hydrogel scaffolds were cultured with HDFs and evaluated using a live/dead assay to assess any cytotoxic effects after 24 h of incubation. As shown in Figure 8(a,b), minimal to no cytotoxic effects were observed. Green staining indicates live cells, while red staining represents dead cells. Across both 9GE and 9GE_0.05ASI formulations, only a small number of dead cells (red staining) were detected, as seen in Figure 8b a, demonstrating their biocompatibility and low cytotoxicity towards HDFs. The quantitative

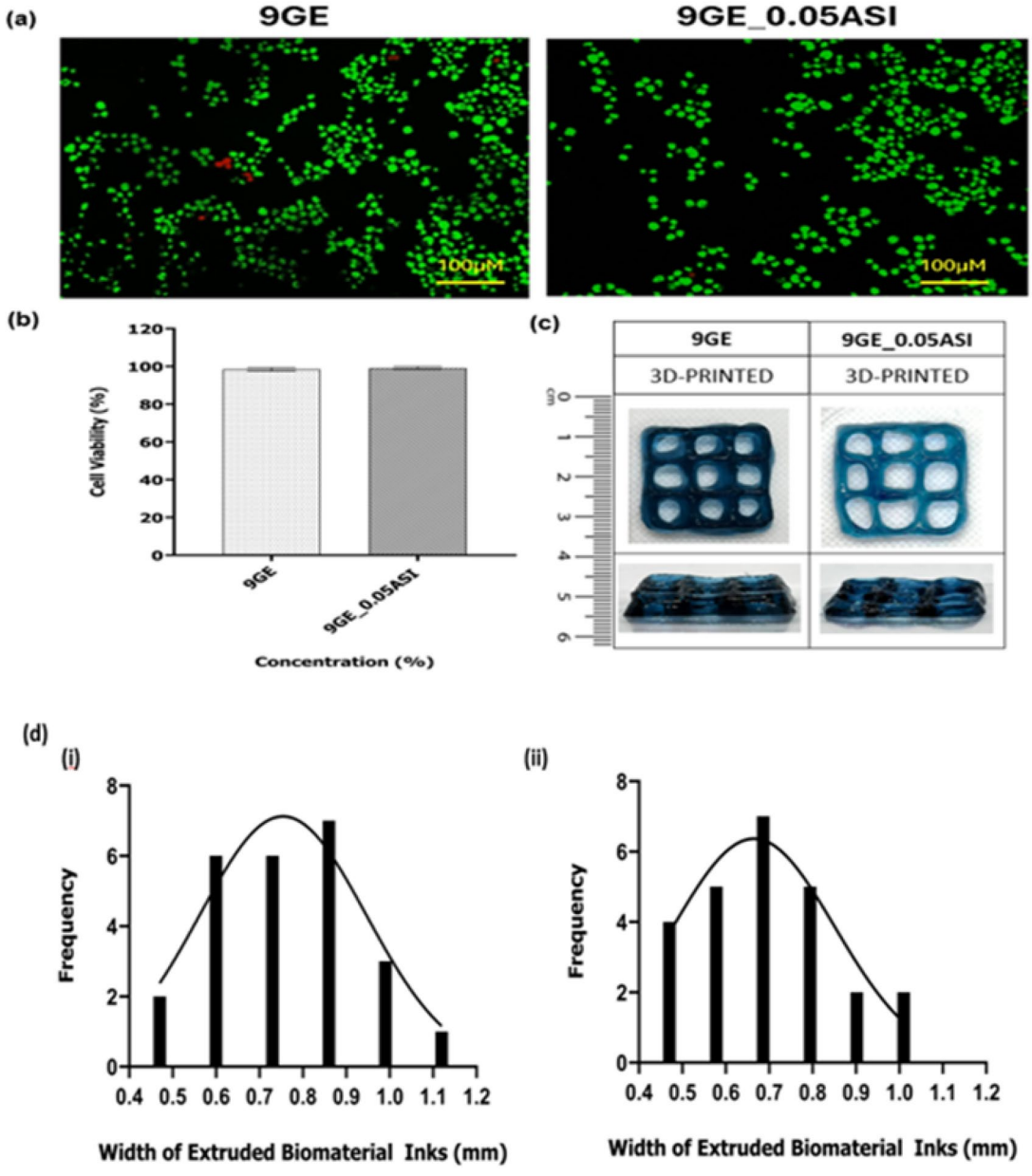

Figure 8. (**a**) Live and dead assay and cytotoxicity assessment of HDFs towards hydrogels (**b**) cell viability of HDFs on hydrogel scaffolds **(c)** gross appearance of top and side view on 3D-printed 9GE and 9GE_0.05ASI hydrogel scaffolds (**d**) Width distribution graph for quantitative assessment of printability; (**i**) 9GE (**ii**) 9GE_0.05ASI. Images for live and dead assay was the best sample chosen from $N = 3$ independent biological replicates, with $n = 5$ technical replicates per condition whereas data for cell viability represents mean ± SD of $N = 3$ independent biological replicates, with $n = 5$ technical replicates per condition. As for 3D-bioprinted images best sample was chosen from $N = 3$ independent fabrication batches, with $n = 5$ technical replicates per condition while width distribution graph was mean ± SD of $N = 3$ independent fabrication batches, with $n = 5$ technical replicates per condition.

results in Figure 8(b) further confirm the excellent biocompatibility of both hydrogels, with cell viability values close to 100%. Specifically, 9GE_0.05ASI showed a slightly higher cell viability of 99.13 ± 0.81% compared to 98.48 ± 0.87% for 9GE.

The hydrogel formulations were assessed as potential biomaterial inks for future 3D bioprinting applications using an extrusion-based method at room temperature (24 °C). Figure 8(c) shows the overall appearance of the printed hydrogels at both top and side view for 9GE and 9GE_0.05ASI formulations showing the printability of both formulations. Printing was performed with an extrusion-based system, where pressure regulators and a fixed speed of 2000 mm/s controlled the material flow through a 0.4 mm nozzle. The blue-coloured hydrogels were also crosslinked during the fabrication process before printing. To complement the qualitative visualization of printed constructs, quantitative printability parameters were evaluated, including extrusion pressure and filament width distribution, which are commonly used metrics for assessing extrusion-based biomaterial inks. The quantitative assessment of print fidelity and filament uniformity revealed distinct differences between 9GE and 9GE_0.05ASI formulations. The width distribution analysis also revealed distinct differences between the 9GE and the asiaticoside-loaded hydrogel (9GE_0.05ASI). In 9GE, the width distribution graph showed a broader and right-skewed distribution, with the modal value centred around 0.8–0.85 mm and occasional strands reaching up to 1.1 mm corresponding to a print fidelity of 208% relative to the 0.4 mm nozzle diameter, indicating substantial post-extrusion spreading. This variability suggests inconsistent extrusion behaviour, likely influenced by die-swell or post-deposition spreading, which compromises printing precision. In contrast, the incorporation of 0.05% asiaticoside shifted the distribution towards smaller widths, with the mode at approximately 0.7 mm, yielding a print fidelity of 175%, significantly improved dimensional accuracy and narrowed the overall spread, resulting in a more uniform and controlled output. Filament uniformity was also enhanced by asiaticoside incorporation, as evidenced by a lower coefficient of variation (CV) for 9GE_0.05ASI (11.4%) compared to 9GE (18.1%), demonstrating more consistent extrusion behaviour. Thus, 9GE_0.05ASI formulation exhibited a narrower and more symmetric filament width distribution compared to the control 9GE, indicating more consistent filament formation and reduced variability during extrusion. In contrast, the broader distribution observed for 9GE, including a higher frequency of wider filaments, suggests greater post-deposition spreading and less stable extrusion behaviour. These results demonstrate that asiaticoside incorporation improves filament uniformity and enhances print fidelity under identical printing conditions.

Although direct extrusion pressure was not measured due to instrument limitations, rheological analysis demonstrated that 9GE_0.05ASI possessed significantly lower complex viscosity and yield behaviour compared to 9GE, indicating a reduced extrusion pressure requirement. This relationship between viscosity and extrusion pressure has been well established in extrusion-based bioprinting systems [30,45].

Cell migration assessment using scratch assay

The effect of asiaticoside incorporation on HDFs migration was evaluated using an *in vitro* scratch wound healing assay. Figure 9(a) presents representative phase-contrast images of HDFs treated with 9GE and 9GE_0.05ASI over a 5-day period (Day 0, 1, 3, and 5) with the initial scratch starting on Day 0. The initial scratch width at Day 0 was comparable across all groups, confirming consistent wound creation and ensuring reliable comparison of wound closure rates.

In the control 9GE group, gradual cell migration into the denuded area was observed over time. Partial wound closure was evident by Day 1, with a noticeable reduction in scratch width by Day 3. Complete or near-complete closure was achieved by Day 5, indicating that gelatin-based hydrogels without asiaticoside are inherently supportive of fibroblast migration and proliferation. In contrast, the asiaticoside-loaded formulation, which is 9GE_0.05ASI demonstrated accelerated wound closure kinetics at all evaluated time points. As early as Day 1, fibroblasts exposed to 9GE_0.05ASI showed more extensive migration into the scratch region compared to the control. By Day 3, the wound gap in the asiaticoside group was substantially narrower, with cells forming a denser and more continuous monolayer across the scratched area. By Day 5, near-complete closure was achieved, with minimal residual gap visible.

Quantitative analysis of wound healing progression is presented in Figure 9(b). At Day 1 (D1), partial wound closure was observed in both groups. The control hydrogel 9GE demonstrated approximately 65-70% wound closure, while the asiaticoside-loaded hydrogel 9GE_0.05ASI exhibited approximately 50-55% closure. Although a numerical difference was observed at this early time point, statistical analysis indicated no significant difference between the two treatment groups, suggesting comparable initial HDFs migratory response following scratch induction.

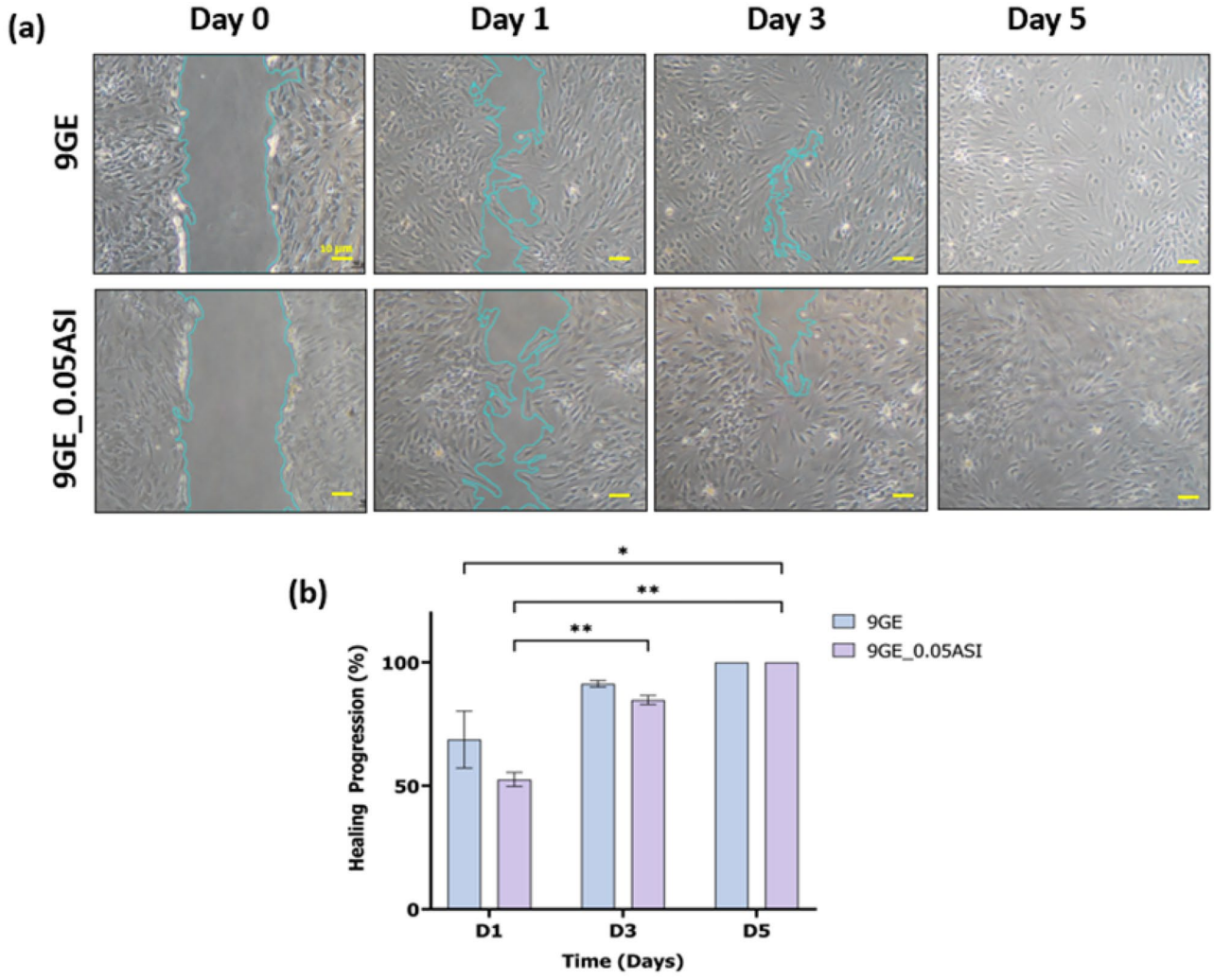

Figure 9. (a) Scratch assay using HDFs exposed to hydrogel leachate media, with the wound area imaged at 40x magnification on Day 1, Day 3, and Day 5 (b) Quantification graph of the healing progression (%) representing the migration rate. *Indicates $p < 0.05$ where $p = 0.0108$, and ** indicates $p < 0.01$ where $p = 0.0011$. Data represents mean ± SD of $N = 3$ independent biological replicates, with $n = 5$ technical replicates per condition. A significant main effect of addition of ASI on healing progression with very large effect size where $\eta p^2 = 0.93$, whereas the main effect of incubation time was less significant but still large effect size where $\eta p^2 = 0.35$.

By Day 3 (D3), a substantial increase in wound closure was evident in both groups, indicating active fibroblast migration into the scratched region. The 9GE group achieved approximately 90-95% wound closure, while the 9GE_0.05ASI group reached approximately 85-90%. When compared to Day 1, 9GE_0.05ASI group showed a statistically significant enhancement in wound closure where ** is $p < 0.01$ and $p = 0.0011$, confirming a significant time-dependent healing progression of cell migration during the intermediate healing phase.

At Day 5 (D5), complete wound closure was achieved in both experimental groups, with wound healing percentages of 100% for both group signalling fully migrated HDFs into the scratched (wounded) region. Statistical comparison revealed that the wound closure observed at Day 5 for the asiaticoside-loaded hydrogel was significantly higher when compared to the Day 1 control group 9GE where $*\boldsymbol{p} < 0.05$ and $\boldsymbol{p} = 0.0108$, indicating a sustained improvement in wound healing progression over time. As for control group and asiaticoside-loaded hydrogel, no statistically significant difference was observed between the two groups at Day 5, suggesting convergence towards complete wound closure at the late stage of the assay.

Overall, the quantitative scratch assay results demonstrate a clear time-dependent increase in fibroblast migration for both hydrogels as the effect size of the incubation time is large where $\eta p^2 = 0.35$. Importantly, the asiaticoside-loaded formulation exhibited statistically significant improvement in wound healing progression across the experimental duration,

supporting its role in sustaining fibroblast migratory activity during *in vitro* wound closure with a main significant effect due to the very large effect size of $\eta p^2 = 0.93$. These findings also indicate that suggesting that the pro-migratory effect of asiaticoside is sustained over time rather than limited to early-stage healing.

Discussion

To address the significant therapeutic challenge posed by chronic wounds, a condition with a global prevalence ranging from 2.00 to 3.55 per 1,000 people, our study investigates the formulation of a unique biomaterial ink as a promising medium for enhancing chronic wound healing [9]. The effects of adding asiaticoside and crosslinking with genipin on the physicochemical and mechanical characteristics of distinct hydrogel samples was examined. Each of the hydrogel groups exhibited unique outcomes in terms of their polymerization process, physical and chemical properties, tensile strength, and chemical makeup. A dose-response analysis revealed that the viability of fibroblast cells differed among the samples, indicating that the inclusion of asiaticoside affected cellular reactions. A cell attachment analysis highlighted the favourable role of ASI in cellular adhesion. Variations in gelation time between the groups demonstrated that ASI was a factor in the gelation process. Further investigation into the hydrogels' physicochemical and tensile qualities revealed that ASI impacted their ability to swell, their stability, and their overall structure. The success of the crosslinking was confirmed through chemical analysis, and measurements of microporosity offered insights into how the hydrogels might influence cell behaviour. These results lay the groundwork for a more in-depth discussion about the effects of asiaticoside addition and genipin crosslinking, particularly regarding their potential use in treating cutaneous tissue loss. This section will explore these findings in greater detail, considering their significance and wider implications.

Asiaticoside's effect on human dermal fibroblasts (HDFs)

Based on the findings found in this study, significant insights on effects of different asiaticoside concentrations on fibroblasts viability over periods of time. Lower asiaticoside concentrations of 0.01% w/v and 0.05% w/v were found promoting cell proliferation as the cell viability was above 100% at 24 h and 48 h for 0.01% w/v and 24 h for 0.05% w/v. This supports existing literature that indicates asiaticoside promotes cell proliferation by stimulating fibroblasts and enhancing the synthesis of collagen providing anti-inflammatory and antioxidant benefits [48]. However, at higher concentrations (0.5% w/v and 1.0% w/v), a significant reduction in cell viability was observed. At 0.5% w/v, the decline became evident especially at the 48-h and 72-h time points, with viability dropping close to 0% at 72 h, suggesting pronounced cytotoxic effects. The cytotoxicity was even more pronounced at 1.0% w/v, where fibroblasts viability dropped drastically across all time points, falling below 50% and reaching complete loss of viability at 72 h. This aligns with previous studies that demonstrated higher concentrations of asiaticoside led to reduction in cell viability of HDFs directly imposing inhibitory effect on cell growth and survival [49].

There are several factors that are attributed to the cytotoxicity of asiaticoside at higher concentrations. The high production of reactive oxygen species (ROS) by asiaticoside at higher concentration is one of the possible mechanisms that led to the reduction in the cell viability [49]. The regulation of oxidative stress is particularly critical in diabetic wound management. Recent studies on metal-polyphenol nanocomposite hydrogels have demonstrated that scavenging excessive reactive oxygen species (ROS) and reprogramming the metabolic microenvironment are essential strategies for treating diabetic foot ulcers [50]. This supports our observation that a precise therapeutic window is required as such at higher doses, asiaticoside acts as a pro-oxidant, generating a level of ROS that completely overwhelms the fibroblasts' natural antioxidant defences ultimately reducing the viability. Asiatic acid in asiaticoside at high levels caused this high level of ROS leading to reduction cell viability. The decline in cell viability over long exposure across almost all concentrations indicate gradual buildup of reactive oxygen species (ROS) that intensifies the cytotoxic effect even at moderately high concentrations of asiaticoside [49].

Successful fabrication and crosslinking of hydrogels

To overcome the shortcomings of existing treatments and enable the functional regeneration of skin, progress in tissue engineering for wound healing is paramount. These developments are concentrated on the creation of biomaterial inks that offer enhanced biocompatibility, effectively replicate the natural

extracellular matrix, and preserve cell viability throughout the bioprinting process. Specifically, such biomaterial inks must have the right mechanical characteristics to endure physiological stress, enable the formation of blood vessels and skin appendages for complete functionality, and be simple to print for the accurate construction of elaborate skin structures [51]. Therefore, this study's objective is to engineer an ideal injectable hydrogel that is polymerizing and non-toxic, rendering it appropriate for cell-based therapies and a prospective biomaterial ink for future applications in 3D bioprinting.

From a chemical perspective, gelatin is a denatured collagen-derived biopolymer composed mainly of glycine, proline, and hydroxyproline residues, with an approximate molecular formula repeating unit of $C_{102}H_{151}O_{39}N_{31}$ [52,53]. The polymer backbone contains abundant functional groups, including primary amines ($-NH_2$), carboxyl (-COOH), and hydroxyl (-OH) groups, which serve as reactive sites for crosslinking. Genipin with molecular formula of $C_{11}H_{14}O_5$ is a naturally occurring iridoid monoterpenoid containing a reactive dihydropyran ring and ester functional groups, enabling it to act as an efficient crosslinking agent for protein-based polymers [54]. Asiaticoside is a pentacyclic triterpenoid saponin with the molecular formula $C_{48}H_{79}O_{19}$, composed of a hydrophobic triterpene aglycone conjugated to hydrophilic sugar moieties rich in hydroxyl groups [55]. During hydrogel fabrication, gelatin constitutes the primary polymeric network, genipin functions as the chemical crosslinker, and asiaticoside is incorporated as a bioactive compound with biological functionality within the hydrogel matrix.Due to the polymeric and crosslinked nature of the gelatin-genipin system, the hydrogel does not possess a single discrete molecular formula. Instead, its chemical structure is best represented as a repeating gelatin polypeptide unit interconnected by with genipin creating covalent bonded crosslink. In the crosslinked hydrogel, gelatin chains are joined through newly formed Schiff-base (C=N) linkages and secondary amide (C–N) bonds originating from reactions between gelatin ε-amino groups and genipin's reactive dihydropyran and ester functionalities. Accordingly, the chemical formula of the hydrogel can be expressed as a network structure comprising repeating gelatin units $C_{102}H_{151}O_{39}N_{31}$ bridged by genipin ($C_{11}H_{14}O_5$), with the presence of newly formed C=N and C–N bonds defining the crosslinked architecture. Asiaticoside with formula of $C_{48}H_{79}O_{19}$ is incorporated within this network without altering the covalent backbone, remaining physically entrapped through hydrogen bonding and intermolecular interactions.

This study reports the successful formulation of hydrogels from combinations of a natural polymer, gelatin, and asiaticoside, which exhibit promising therapeutic efficacy for chronic skin wounds. Genipin was also included to boost the hydrogel's structural stability and to stimulate cellular proliferation, thereby enhancing wound repair [56]. Among the various formulations, 9GE_0.05ASI (9% w/v gelatin, and 0.05% w/v asiaticoside) and 10GE_0.05ASI (10% w/v gelatin, and 0.05% w/v asiaticoside) were pinpointed as optimal. These formulations feature a three-minute gelation time at ambient temperature, a rate that is slow enough to permit adequate time for clinical application before setting [31], yet fast enough to prevent premature solidification that would complicate extrusion in 3D bioprinting. The presence of genipin enables this controlled timing by forming covalent crosslinks with the amino-polymeric elements within the gelatin [57].

The formation of the gelatin-genipin hydrogel is governed predominantly by covalent bonds crosslinking reactions between genipin and the free amino groups of gelatin. The interaction between gelatin and genipin for hydrogel formation is understood to proceed *via* two main reaction routes. The first involves a nucleophilic attack on the C-3 carbon of the genipin molecule by the free amino groups present in gelatin which is primarily the ε-amino groups of lysine residues [57]. This attack induces the opening of the dihydropyran ring within the genipin structure, ultimately leading to the formation of a continuous, interconnected gelatin network that reinforces the hydrogel's mechanical properties and overall stability. In the second route, a reaction occurs between the gelatin's amino groups and the genipin's carboxyl group, forming stable amide bonds [57]. These covalent amide linkages act as crosslinks, significantly strengthening the hydrogel and enhancing its resistance to enzymatic or chemical degradation. These mechanisms work in concert to create a robust, crosslinked network, which is key to the hydrogel's improved mechanical strength and durability. Furthermore, an additional reaction, the oxygen radical-induced polymerization of genipin, can also take place. This contributes to the further stabilization of the hydrogel matrix and is accompanied by the development of a characteristic blue colouration, which serves as a visual confirmation of successful crosslinking [57]. The controlled development of this intricately crosslinked architecture is crucial for producing a hydrogel that is both structurally sound and sufficiently elastic for various biomedical uses.

Physical properties and effects on wound healing

Characterizing hydrogels' physicochemical properties allow for an ideal evaluation of hydrogels' performance. Evaluating the hydrogels' capacity for fluid absorption was a crucial first step in evaluating their functional viability for clinical wound care as wounded skin would lose a notably large amount of moisture and water. As for the fabricated gelatin-based hydrogels, whether with or without ASI, an optimal and acceptable swelling ratio was observed, allowing all formulations to effectively manage excess wound exudate at the injury site. It was observed that all formulations showed a swelling ratio of above 500%, particularly ASI-loaded hydrogels, making them ideal to be used for wound healing applications. Gelatin, as a major component, naturally displays hydrophilic properties owing to its polar amino acid residues, which include functional groups like hydroxyl (-OH), carboxyl (-COOH), and amine (-NH2) [51]. These groups actively interact with water through hydrogen bonding, enabling the gelatin-genipin hydrogel matrix to initially absorb and retain moisture. Comparing the highest swelling capacity formulation with lowest swelling ratio formulation shows that addition of asiaticoside into the gelatin-based hydrogel formulation significantly increased the swelling capacity. This shows that incorporation of asiaticoside even at low concentration (0.05% w/v) markedly improves the hydrogels' swelling ability and being well above 500% in retaining water. This capacity helps manage wound exudate while ensuring effective fluid absorption which was primarily caused by the hydroxyl (–OH) groups existing in asiaticoside, making asiaticoside overall amphiphilic but strongly hydrophilic on its surface [58]. In a hydrogel, these sugar -OH groups act like water attractants, forming hydrogen bonds with surrounding water. By contrast, the gelatin polymer itself is hydrophilic, containing -OH, -COOH and -NH2 residues and readily bonds with water [59]. Thus, embedding asiaticoside into gelatin further enriches the network with polar, water-attracting sites. In analogous systems, addition of sugar-rich additives such as honey has been shown to dramatically enhance water uptake. For instance, a gelatin–genipin hydrogel with 0.1% w/v Kelulut honey swelled to ~742% of its dry weight versus ~692% without honey [59]. By the same token, asiaticoside's sugar units are expected to increase hydrophilicity and swelling.

The incorporation of ASI into the composite gelatin-based hydrogel scaffolds is shown to be an effective strategy for enhancing the hydrogels' surface hydrophilicity [58]. The contact angle measurements provide direct evidence of how ASI incorporation improves the wettability of the gelatin-based hydrogel. While all formulations exhibited a hydrophilic nature with contact angles below 90°, a statistically significant decrease in the contact angle was observed upon the addition of ASI to the more concentrated gelatin formulation. Asiaticoside structure carries multiple polar hydroxyl and glycosidic oxygen groups on its sugar moiety. When asiaticoside is incorporated into a gelatin-genipin hydrogel, its polar sugar units are exposed at the polymer interface. These hydroxyl-rich regions can form hydrogen bonds with water, effectively raising the surface energy of the hydrogel. Increasing the solid's surface energy makes the surface more attractive to water, thus lowering the equilibrium contact angle θ [59]. In practice, loading hydrophilic additives is known to shrink contact angles, for example, adding sugar-rich Kelulut honey to gelatin-genipin hydrogels consistently lowered their contact angles (from ~60° down to ~42°) by introducing abundant -OH groups that bond with water.

In addition, an adequate WVTR level is required for hydrogels to maintain the optimal moisture content surrounding the wound area. WVTR acts as an important factor in wound healing applications by ensuring the wound area stays moist. An ideal WVTR for a skin substitute is considered to be over 1500 g/m^2/h to ensure the wound remains hydrated without becoming excessively dry [60]. All the gelatin-genipin hydrogels created in this study as can be seen in Figure 4c, including those with and without asiaticoside, demonstrated favourable WVTRs that fall within the effective range for hydrogels, promoting a healthy moisture balance despite the significant reduction in WVTR caused by addition of asiaticoside into 9GE and 10GE formulations. The results indicate that despite variations in the concentrations of asiaticoside and gelatin, the changes in crosslinking density did not substantially affect the overall performance of water vapour permeability, even though there might have been alterations to the hydrogel's pore structure.

Furthermore, *in vitro* biodegradation of the hydrogel formulations is another important factor that needs to be tested and considered for the intended wound healing applications. The reason this is such a critical aspect to evaluate is that a rapid rate of biodegradation of the biomaterials after they have been implanted onto the wound site has been identified as a currently existing issue with other hydrogel formulations that are available. The control hydrogels that did not contain ASI exhibited relatively low degradation rates. It was observed that the addition of 0.05% w/v ASI slightly reduced the degradation rate in the formulations. However, this reduction was found to be comparable to the control (9GE and 10GE) formulations. For

a hydrogel to be deemed ideally selected for wound healing applications, it is expected to remain structurally intact for a minimum duration of 14 days before it undergoes complete degradation at the site of implantation. This requirement corresponds to a maximum allowable degradation rate of 0.2 mg/h [61]. These latest findings suggest that the effect of asiaticoside on the biodegradation rate of the formulations is minimal, yet it is still noticeable in its ability to reduce the degradation rate of the non-ASI-incorporated hydrogel. Nevertheless, it is crucial that all of the hydrogel formulations tested, including those containing ASI, successfully maintained a biodegradation rate well below 0.1 mg/h. This outcome serves as confirmation that the hydrogels degrade in a controlled and predictable manner, which is a characteristic that makes them highly suitable for providing the sustained and continuous support needed during the wound healing process.

Mechanical properties and their significance

As displayed in Figure 5, compression and resilience were tested on the hydrogel formulations to assess the mechanical integrity of the hydrogels for the purpose of wound-healing application. It was found that all formulations have comparable compression percentage as can be seen in Figure 5(a) that proofs addition of asiaticoside did not significantly affect how the hydrogels respond to pressure. Similarly, the resilience of the hydrogels, which is their ability to return to their original shape after being deformed, remained largely consistent across all formulations. This consistency suggests that even at concentrations up to 0.05% w/v, asiaticoside does not cause significant changes to the hydrogel's elastic properties, which are governed by the density of the polymer network's crosslinks and the mobility of its polymer chains. Although minor fluctuations in compression were noted, such as a slight dip in the sample containing 0.05% w/v asiaticoside (9GE_0.05ASI, and 10GE_0.05ASI), these were not deemed statistically significant (Figure 5a). Therefore, the inclusion of asiaticoside at the tested concentrations does not compromise the fundamental mechanical behaviour of the hydrogels, preserving their suitability for applications in tissue regeneration.

Although no statistically significant differences were observed in compression and resilience among the hydrogel formulations, these findings remain highly relevant in the context of wound-healing biomechanics. For wound healing applications, an ideal scaffold must provide sufficient mechanical stability to protect the wound bed while maintaining tissue compliance that allows the material to deform synchronously with surrounding skin during movement. Excessively stiff materials can impede cellular migration and cause patient discomfort, whereas overly soft scaffolds may collapse under physiological stresses, compromising wound coverage and healing outcomes [62]. The comparable compression and resilience observed across all formulations indicates that incorporation of asiaticoside does not weaken the structural integrity of the gelatin-genipin network. This mechanical stability is essential for maintaining scaffold thickness and protecting newly forming tissue from external mechanical forces such as shear, compression, and friction from dressings or clothing. At the same time, the high resilience values demonstrate the hydrogels' ability to recover their original shape following deformation, a property that is particularly important for wound sites exposed to repetitive mechanical loading caused by skin stretching, joint movement, or body motion [63].

From a biomechanical perspective, the combination of high compressive strength and near-complete shape recovery suggests that the hydrogels exhibit skin-like elastic behaviour rather than rigid, load-bearing characteristics. Such compliance allows the material to conform to dynamic wound geometries without mechanical failure. Importantly, the preservation of these properties after asiaticoside incorporation confirms that the bioactive modification does not compromise the hydrogel's mechanical compatibility with native skin tissue [62–64]. The stability of these mechanical properties is highly important for wound healing. It confirms that the bioactive components of asiaticoside can be incorporated without disrupting the hydrogel's underlying polymer structure. These mechanical attributes are vital for providing a supportive framework for new tissue growth and promoting the necessary movement and growth of cells [63]. The fact that these properties are preserved highlights the hydrogel's potential as a durable and biocompatible scaffold for regenerating tissue. It is essential that the hydrogel's mechanical characteristics, such as elasticity and flexibility, mimic those of the native tissue it is intended to replace, ensuring proper integration and function during the healing process [63].

Rheological tests were also conducted as observed in Figure 5(c–e), which include complex viscosity, storage modulus, and loss modulus results. Addition of rheological analysis to the mechanical properties of the hydrogels allow for more in depth and comprehensive profiling and understanding of the hydrogel's formulations and their suitability for wound healing applications. The initial compression and resilience tests established that the fundamental structural integrity and elastic nature of the hydrogel are robust

enough to withstand the inclusion of bioactive agents like asiaticoside without significant mechanical stability reduction. This confirmed the hydrogel's basic viability as a physically stable material capable of providing the necessary support for regenerating tissue.

A key indicator of hydrogel stability is when the storage modulus (G′) is substantially greater than the loss modulus (G′′) [64]. Both the 9GE and 9GE_0.05ASI formulations consistently demonstrate a solid-like behaviour (G′ > G′′) throughout the frequency range. This result is significant as it verifies the successful development of a stable, crosslinked 3D network that can retain its structural integrity under application. Such stability is critical for withstanding mechanical stress within the wound site while providing a long-lasting framework that supports cell adhesion, migration, and proliferation, thereby replicating the role of the native extracellular matrix (ECM).

Both hydrogel formulations exhibit strong shear-thinning characteristics, demonstrated by the sharp decline in complex viscosity (η∗) as the angular frequency increases as can be seen in Figure 5e [65]. This rheological profile is typical of an ideal bioprinted biomaterial ink. When at rest or exposed to low shear stress, such as within a wound site, the hydrogel retains high viscosity, which prevents it from leaking out of the defect. In contrast, under the high shear stress encountered during syringe injection, its viscosity decreases markedly, enabling smooth administration. This ability to temporarily fluidize during injection and rapidly recover afterward is particularly beneficial for clinical applications, as it supports minimally invasive delivery while ensuring the material adapts to and remains within complex wound shapes [65].

The addition of 0.05% w/v asiaticoside leads to a distinct alteration in the hydrogel's mechanical characteristics. A consistent decline in complex viscosity, storage modulus, and loss modulus suggests that asiaticoside acts as a molecular plasticizer within the gelatin-genipin network [58]. Given its relatively small triterpenoid structure, asiaticoside is thought to intercalate between gelatin chains, interfering with intermolecular hydrogen bonding and partially obstructing genipin-mediated cross-linking. This increases the available free volume and enhances chain mobility, ultimately producing a hydrogel that is mechanically softer and more flexible. This asiaticoside-induced softening is not a detriment but rather a potentially significant therapeutic advantage. A lower storage modulus translates to greater flexibility, which can enhance the hydrogel's ability to conform adhesively to the complex and irregular topography of a wound bed. This improved conformability ensures complete contact between the dressing and the tissue, eliminating dead space where wound exudate could pool and bacteria could proliferate.

Together, these data demonstrate that both formulations combine injectable shear-thinning (low η* at high rad/s) with strong gel-like behaviour under low shear (G′ > G″). Incorporation of 0.05% w/v ASI gently attenuates viscosity, elasticity, and viscous dissipation, making the hydrogel softer and more deformable, without compromising its overall solid-like character and the ability to withstand pressure and maintain original shape under pressure. Such tuneable viscoelastic properties are advantageous for a wound-healing scaffold that must be administered through a syringe yet retain its shape and mechanical integrity once in place. When compression and resilience are being considered alongside the rheological results, which demonstrate shear-thinning behaviour and reduced storage modulus in asiaticoside-loaded formulations, the mechanical data collectively suggest a balanced biomechanical profile. The hydrogels remain sufficiently robust to withstand handling and *in situ* stresses, while retaining the flexibility needed to accommodate physiological skin deformation. This balance is critical for wound dressings and injectable scaffolds intended to remain in contact with the wound bed throughout the healing process, supporting tissue regeneration without inducing mechanical irritation or stress shielding.

Chemical and structural characterization

FTIR spectroscopy results observed in Figures 6 explores the key functional groups that exist in the hydrogel related to the components which are gelatin, genipin, and addition of ASI. In the FTIR spectra of the gelatin-genipin hydrogels, the Amide A region (N-H/O-H stretch) shows a broad band that shifts from ~3280 cm − 1in pure gelatin down to ~3260 cm^{-1} upon crosslinking. This red-shift and broadening indicate new hydrogen-bonding interactions between gelatin's amine/hydroxyl groups and genipin proving successful crosslinking [59]. This aligns with a study that found adding genipin shifts the N-H/O-H band to lower wavenumbers due to increased hydrogen-bonding in the network [66]. Notably, the CH band pattern is essentially unchanged by adding ASI, consistent with ASI being physically entrapped rather than covalently bonded.

Finally, the ASI-specific signatures appear in the fingerprint region. In ASI-loaded gels we observe new weak bands around 1030–1080 cm^{-1}, which are assigned to C-O stretching of the glycosidic sugar

moieties in asiaticoside. FTIR analysis of polysaccharides and glycosides typically shows strong C-O-C and C-O bands in this range [59]. The appearance of these bands only in ASI-containing samples confirms that the triterpenoid saponin is incorporated. Additional broad features below 1000 cm^{-1} match known triterpene vibrations. Overall, these new absorptions coupled with the fact that no new covalent peaks (other than the Schiff-base) are seen, indicate that asiaticoside is physically entrapped in the hydrogel network and held by hydrogen bonds.

In summary, the FTIR data confirm successful genipin crosslinking of gelatin (*via* Schiff-base imine formation) and show that asiaticoside is incorporated through non-covalent entrapment. The observed N-H/O-H and amide I/II shifts agree with literature reports of genipin-gelatin chemistry while the emergence of C-O peaks in the 1030–1080 cm^{-1} range and other fingerprint bands verify the presence of the sugar-containing asiaticoside [58,59].

Results show that 10GE_0.05ASI contains the highest amorphous fraction, while 9GE_0.05ASI has the lowest. This trend is expected because the amorphous portion of a hydrogel is simply calculated as 100% minus crystallinity. The amorphous domains are disordered and water-rich as they largely govern swelling behaviour, flexibility, and molecular diffusion pathways [67]. In contrast, crystalline regions are more compact and ordered, contributing mainly to rigidity and structural strength. Each structural feature plays a distinct functional role. Crystalline regions act as strong physical crosslinks, reinforcing the hydrogel, enhancing its elastic modulus, and resisting deformation. Stacked or folded chain arrangements also help prevent crack propagation, providing toughness. Meanwhile, the amorphous matrix ensures flexibility and high-water uptake, forming a hydrated mesh that retains water and supports nutrient or drug diffusion [67]. A balance between these two domains is crucial. Too little amorphous content results in a hydrogel that is overly rigid or brittle, while too much amorphous fraction (with reduced crystallinity) can make it weak and unstable. In our study, 9GE_0.05ASI, appears to maintain a favourable balance between strength and permeability. On the other hand, 10GE_0.05ASI, is likely to swell more extensively but at the cost of lower mechanical robustness.

EDX analysis was performed to determine the elemental composition of gelatin-genipin hydrogels including incorporation of asiaticoside into the hydrogel formulations. Both gelatin-only scaffolds (9GE and 10GE) showed comparable elemental distributions of carbon, oxygen, and nitrogen, consistent with the proteinaceous nature of gelatin. Incorporation of 0.05% asiaticoside into 9GE (9GE_0.05ASI) resulted in a reduction in carbon content, while oxygen and nitrogen levels showed slight increases. A similar but more pronounced trend was observed in 10GE_0.05ASI, with carbon decreasing further and oxygen and nitrogen contents increasing.

These variations confirm the successful incorporation of asiaticoside into the hydrogel matrix. The decrease in carbon likely reflects partial substitution of gelatin's carbon-rich protein backbone with asiaticoside's hydroxyl-rich glycosidic structures, which contribute higher oxygen content [58]. The increase in oxygen is attributed to asiaticoside's abundant hydroxyl groups, while the rise in nitrogen suggests possible interactions with gelatin's amino groups, potentially through hydrogen bonding or secondary crosslinking. The greater elemental shifts in 10GE_0.05ASI compared to 9GE_0.05ASI imply that asiaticoside incorporation may depend on crosslinking density or polymer concentration, with higher gelatin content offering more binding sites. Overall, these compositional changes not only verify asiaticoside integration but also emphasize its role in enriching the hydrogel with functional groups that enhance hydrophilicity and biological activity.

Beyond confirming the presence of asiaticoside, the FTIR and XRD findings also provide insight into how ASI's molecular architecture modulates the gelatin–genipin network. Asiaticoside is a triterpenoid saponin composed of a rigid pentacyclic hydrophobic backbone conjugated to multiple sugar moieties rich in hydroxyl (–OH) groups [48,58]. These glycosidic groups introduce a high density of hydrogen-bond donors and acceptors, enabling extensive non-covalent interactions with gelatin's amine ($–NH_2$), carboxyl (–COOH), and hydroxyl (–OH) functionalities. The observed red-shift and broadening of the Amide A and Amide I bands upon ASI incorporation are therefore attributed not only to genipin-mediated crosslinking, but also to additional hydrogen bonding between ASI sugar residues and gelatin chains, which increases intermolecular association without forming new covalent bonds.

At the same time, the bulky triterpenoid backbone of ASI introduces steric constraints within the polymeric network. While genipin primarily crosslinks gelatin *via* Schiff-base reactions with free amine groups, the physical presence of ASI between gelatin chains may partially hinder close chain packing or limit genipin accessibility to some reactive sites. This dual effect of hydrogen-bond reinforcement combined with steric interference, provides a molecular explanation for the altered network organization observed in XRD analysis.

At lower gelatin concentration of 9% w/v, ASI appears to promote local chain ordering through hydrogen-bond-mediated alignment, resulting in increased crystallinity. In contrast, at higher gelatin concentration of 10% w/v, increased chain entanglement together with ASI steric bulk disrupts ordered domain formation, leading to a higher amorphous fraction.

Microporous structure

To characterize the hydrogels formulation for its potential use as a 3D bioprinting biomaterial ink, an investigation was initiated by collecting preliminary data. This process involved a visual assessment of the hydrogel's overall appearance and a detailed analysis of its internal structure. Specifically, the average pore sizes were determined by examining Scanning Electron Microscopy (SEM) micrographs, which are presented in Figure 7. Furthermore, the hydrogel's porosity was quantified using the water displacement method. To understand the surface characteristics of the hydrogel post-printing, its surface roughness was analysed with Atomic Force Microscopy (AFM) images in Figure 7, providing an estimation of the surface roughness of all hydrogel formulations.The scanning electron microscopy (SEM) micrographs reveal the distinct microstructural differences between the plain gelatin-genipin (GE) hydrogels and their ASI-loaded counterparts The control hydrogels, 9GE and 10GE, presented a more compact structure characterized by relatively large, well-defined pores with thick interstitial walls. This architecture is typical of gelatin hydrogels crosslinked with genipin, where covalent bonding organizes the polymer chains into a stable, and denser network [68]. In stark contrast, the incorporation of asiaticoside induced a significant morphological shift, resulting in a finer and more heterogeneous pore structure. Both the 9GE_0.05ASI and 10GE_0.05ASI samples exhibited a network composed of numerous small, irregular cavities interconnected by slender struts. This observation strongly suggests that asiaticoside interferes with the hydrogel's self-assembly and crosslinking process. This structural alteration can be primarily attributed to the molecular properties of asiaticoside. As a bulky triterpene saponin, asiaticoside likely introduces significant steric hindrance during the formation of the gelatin-genipin network [59]. As genipin works to crosslink the gelatin chains, the large and complex asiaticoside molecules may physically obstruct the chains from organizing into larger, ordered domains. This interference forces the formation of a less regular network with smaller interstitial spaces and finer polymer struts.

Quantitative analysis of the scaffold microstructure, shown in Figure 7(c), confirms the observations from the SEM images. The incorporation of ASI led to a significant pore refinement. In the formulations with 9% w/v gelatin, the average pore size decreased dramatically from in the plain 9GE hydrogel compared to 9GE_0.05ASI sample A similar trend was observed in the 10% w/v gelatin groups, where the pore size shrank for 10GE_0.05ASI. The pronounced reduction in pore size is a direct consequence of the structural disruption caused by asiaticoside during gelation, as previously discussed. The bulky molecule's steric hindrance interferes with the organization of the gelatin network, leading to the formation of many small pores instead of fewer large ones [59]. This effect appears to be more pronounced at lower gelatin concentrations (9GE) because the polymer chains are less crowded, allowing the ASI molecules to exert a greater relative influence on the final architecture. This ASI-induced pore refinement has significant and beneficial implications for the scaffold's use in biomedical applications. While large pores are essential for cell infiltration, the creation of a finer porous network dramatically increases the overall surface area available for cell adhesion, proliferation, and interaction [59]. Beyond cellular adhesion, the architecture of the scaffold plays a pivotal role in regulating the wound. Recent findings suggest that hydrogels capable of reprogramming the metabolic microenvironment through optimized structural properties and bioactive release can significantly enhance healing outcomes in diabetic foot ulcers [50]. The refined pore network observed in our ASI-loaded hydrogels may therefore facilitate more controlled diffusion of nutrients and oxygen, contributing to a metabolically favourable environment for regeneration. The resulting average pore sizes fall within the optimal range for fibroblasts attachment and growth, which is critical for wound healing and dermal tissue regeneration. The reduction in porosity in ASI-loaded hydrogels is likely caused by intermolecular bridging. Asiaticoside, a large molecule with numerous polar hydroxyls groups, acts as a non-covalent "molecular staple." It forms multiple hydrogen bonds with adjacent gelatin chains, pulling them closer together into a more compact network before the permanent covalent crosslinking with genipin occurs [58,59].

The mean surface roughness of the hydrogel is positively correlated with the gelatin concentration, which is due to the formation of a denser, more rigid polymer matrix. Conversely, incorporating ASI consistently diminishes surface roughness of the hydrogel formulations. In conclusion, the data indicate that increasing the gelatin concentration increases the surface roughness due to better crosslinking with genipin and a

denser network, while ASI reduces the roughness as it alters the structural network of the hydrogel, contributing to smoother hydrogel surfaces more conducive to cell adhesion and behaviour [59].

Evaluation of cytotoxicity on fabricated hydrogel scaffolds

The live/dead assay clearly shows that both 9GE and 9GE_0.05ASI hydrogels are highly biocompatible. After 24 h of incubation with human dermal fibroblasts (HDFs), almost all cells were stained green (live), with only a few stained red (dead), as shown in Figure 8(a). Correspondingly, Figure 8(b) indicates cell viabilities of ~98.5-99.1% for both scaffolds, demonstrating virtually no cytotoxic effect. According to ISO 10993-5 standards, a viability of ≥70% is considered non-cytotoxic. For the fabricated hydrogel scaffolds, values near 100% are well above this threshold. In other words, essentially all fibroblasts survived on fabricated hydrogels confirming excellent cytocompatibility as such high viability implies that the both scaffolds did not impose significant cytotoxic effects on the HDFs. In another study, it was found that all gelatin hydrogel formulations yielded a high number of live cells and very few dead cells, confirming that the hydrogel supports cell viability and provides non-toxic 3D scaffolds [69]. Our findings align with this study as the live/dead assay as shown in Figure 8(a) display many green cells and only sparse red spots, implying that both 9GE and 9GE_0.05ASI scaffolds are essentially non-toxic to HDFs.

Incorporation of asiaticoside (0.05% w/v) to the 9GE scaffold, forming 9GE_0.05ASI was shown to maintain cell viability. Asiaticoside itself is known for low biotoxicity and is often added to biomaterials ink precisely because it supports tissue repair rather than killing cells and the stains that were used in conducting the assays also did not kill the HDFs [58]. This also aligns with a study that reports asiaticoside promotes fibroblasts migration and proliferation by activating Wnt/β-catenin signalling [58]. Thus, our finding that viability is maintained, or slightly improved, in the ASI-loaded scaffold is in line with this study. High fibroblasts viability on these scaffolds is encouraging for wound-healing applications. HDFs play a central role in skin repair such as depositing collagen, and remodelling tissue, which is why scaffolds must be cytocompatible to be useful. The excellent biocompatibility shown by both 9GE and 9GE_0.05ASI suggests that they provide a safe environment for fibroblasts. The fact that the ASI-loaded scaffold is equally, or slightly more supportive of HDF survival is particularly promising, since asiaticoside is intended to accelerate wound healing.

Although a hemocompatibility assessment which is haemolysis assay was not performed in the present study due to ethical constraints related to blood samples collection, the haemolytic behaviour of the selected biomaterials has been characterized in prior studies. Gelatin-genipin crosslinked hydrogels have repeatedly demonstrated excellent hemocompatibility across different studies. In general, gelatin-based hydrogels have demonstrated excellent hemocompatibility, indicating that gelatin itself is an inherently blood-compatible biomaterial. For example, gelatin methacrylate (Gel-GMA) and Gel-GMA/GO hydrogels have been reported to exhibit extremely low haemolysis ratios of only 0.54% and 0.50%, respectively, together with negligible effects on coagulation parameters, confirming their suitability for wound healing applications [70]. These findings further support the notion that gelatin-based hydrogel systems, regardless of the specific crosslinking strategy, typically do not induce red blood cell lysis and possess intrinsically low haemolytic activity. Consistent with these findings, a study investigating 10% (w/v) gelatin hydrogels crosslinked with 0.5% (w/v) genipin and containing varying concentrations of chondroitin sulphate (0-0.1% w/w), haemolysis assays demonstrated that all formulations exhibited haemolysis rates below the internationally accepted limit of 5% [71].

In comparison, the formulation used in the present study contains 9% (w/v) gelatin and 0.1% (w/v) genipin, representing lower biomaterials concentration. Consequently, the haemolysis rate is expected to be lower and remain well within the acceptable 5% threshold. Similarly in another study investigating hydrogels composed of 7% gelatin and 9% alginate, crosslinked with genipin at concentrations of 0%, 0.1%, 0.5%, and 1%, reported that formulations containing lower genipin concentrations (0.1-0.5%) exhibited haemolysis rates below 5%[72]. These findings indicate that genipin at lower concentrations, comparable to the 0.1% used in the present study, is associated with low haemolytic activity and is therefore suitable for wound healing applications. In addition to the favourable hemocompatibility profile of the gelatin-genipin network, the inclusion of asiaticoside is unlikely to introduce haemolytic risk. Asiaticoside is a major bioactive constituent of *Centella asiatica*, which has been extensively evaluated using human red blood cell (HRBC) membrane stabilization assays. Notably, *Centella asiatica* extracts have been shown to inhibit haemolysis achieving up to 94% inhibition at higher concentrations of 2000 µg/mL. This pronounced membrane-stabilizing effect indicates a strong cytoprotective action towards red blood cells. Therefore, the incorporation of asiaticoside is expected to be

hemocompatible rather than compromising blood compatibility.

Evaluation of 3D-bioprinting

The main objective of this study was to evaluate the appropriate composition of hydrogels as potential biomaterial inks for 3D bioprinting. To begin, the hydrogels' visual characteristics were optimized, as shown in Figure 8(c). Results demonstrated that addition of asiaticoside improved performance at room temperature due to its higher viscosity and rapid transition from a semi-solid to a solid state while being able to be extruded from 3D-bioprinter nozzles without any form or clogging. Although both 9GE and 9GE_0.05ASI formulations which are gelatin-based hydrogels showed printability properties, its reversible sol-gel transition can lead to degradation within hours when exposed to growth media at 37 °C. To overcome this, genipin was added to allow crosslinking between gelatin and genipin chains allowing for the hydrogels to maintain the shape once polymerized. This modification enhanced structural stability and prevented hydrogel melting under physiological conditions. Additionally, the use of an extruder and controlled printing platform allowed precise regulation of printing temperature. Altogether, these results highlight the hydrogel's potential as a reliable biomaterial ink for accurate and efficient 3D bioprinting. In terms of width distribution graph in Figure 8(d), the reduction in right-tail outliers in Figure 8(d) (ii) indicates that asiaticoside minimized abnormal filament thickening, suggesting enhanced rheological stability during extrusion. These findings imply that asiaticoside contributes to the production of thinner and more consistent filaments, potentially by reducing die-swell effects and/or promoting faster solid-like recovery after deposition [58]. Consequently, the asiaticoside-loaded hydrogel demonstrates improved resolution, pore-size predictability, and print fidelity, making it a more suitable candidate for fabricating well-defined and reproducible tissue engineering scaffolds.

Beyond qualitative visualization, the quantitative evaluation of print fidelity, filament uniformity provides critical insights into the suitability of the gelatin-asiaticoside hydrogels as biomaterial inks for extrusion-based bioprinting. Print fidelity is a fundamental requirement for any biomaterial ink, as it determines whether the printed construct can accurately replicate the intended geometry and pore architecture, which in turn governs biomaterials diffusion, mechanical integrity, and eventual tissue regeneration [38].

In this study, the asiaticoside-loaded hydrogel (9GE_0.05ASI) exhibited significantly improved print fidelity and filament uniformity compared to the gelatin-only formulation (9GE), as evidenced by its reduced filament spreading, narrower width distribution, and lower coefficient of variation. This improvement suggests that asiaticoside contributes not only biofunctionalities but also favourable rheological modulation, enabling more controlled material deposition. Such behaviour is particularly desirable in wound-healing applications, where conformal coverage and uniform scaffold architecture are essential to ensure homogeneous cellular infiltration and tissue repair.

Although direct extrusion pressure was not measured in this study, the rheological results provide strong indirect evidence regarding extrusion behaviour. The lower complex viscosity and reduced storage modulus of the ASI-loaded hydrogel indicate a lower force requirement for extrusion, which is advantageous for both manual injectability and automated bioprinting systems. It is well established that extrusion pressure in bioprinting is directly related to biomaterial ink viscosity and yield stress, with lower-viscosity, shear-thinning materials requiring substantially less pressure for flow through fine nozzles [65]. Thus, the rheological softening induced by asiaticoside can be interpreted as a printability-enhancing feature rather than a mechanical drawback.

Importantly, this balance between reduced extrusion resistance and preserved solid-like behaviour ($G' > G''$) ensures that the hydrogel remains easy to print while still maintaining sufficient mechanical integrity after deposition. In the context of wound healing, this tuneability is particularly valuable, as it allows minimally invasive delivery through fine-gauge needles while enabling the printed material to retain its shape within irregular wound geometries. Collectively, these findings demonstrate that asiaticoside incorporation improves not only the biological performance of the hydrogel but also its printability and manufacturability, positioning the gelatin-genipin based with loading of asiaticoside system as a promising multifunctional biomaterial ink for extrusion-based 3D bioprinting in wound healing application.

Wound closure analysis

Fibroblast migration is a crucial event during the proliferative phase of wound healing, directly influencing wound gap closure and subsequent extracellular matrix (ECM) deposition. In this study, a scratch wound healing assay was used to investigate the effect of asiaticoside incorporation into a gelatin-based hydrogel

on the migratory behaviour of human dermal fibroblasts (HDFs) as shown in Figure 9. The findings demonstrate that while both hydrogels supported fibroblast migration, the asiaticoside-loaded formulation (9GE_0.05ASI) promoted a more sustained enhancement of wound healing progression over time.

Qualitative observations from phase-contrast images (Figure 9(a)) indicate that the gelatin-based hydrogel alone provides a favourable substrate for fibroblast migration. This is consistent with previous studies reporting that gelatin contains arginine-glycine-aspartic acid (RGD) motifs that facilitate integrin-mediated cell adhesion, cytoskeletal organization, and directional migration of fibroblasts. As a result, gradual wound closure was observed in the control 9GE group, reaching near-complete closure by Day 5. The comparable initial scratch widths across all groups confirm that differences in closure kinetics were attributable to treatment effects rather than experimental variability. Interestingly, asiaticoside incorporation did not result in a statistically significant enhancement of wound closure at Day 1. This observation suggests that asiaticoside does not markedly influence the immediate migratory response following scratch induction. Instead, its effects became more prominent during the intermediate healing phase. Between Day 1 and Day 3, the 9GE_0.05ASI group exhibited a statistically significant increase in wound closure where $\boldsymbol{p} < 0.01$, accompanied by visibly denser and more continuous cell coverage within the scratched region. This temporal pattern is in agreement with previous reports indicating that asiaticoside enhances fibroblast migration and attachment in a time-dependent manner rather than triggering an acute response [48].

The sustained enhancement observed with asiaticoside-loaded hydrogels can be attributed to multiple biological mechanisms. Asiaticoside has been widely reported to stimulate collagen type I synthesis in fibroblasts *via* activation of transforming growth factor-β (TGF-β) signalling pathways, which play a central role in ECM remodelling and wound contraction [48]. Increased collagen deposition not only strengthens the wound matrix but also provides structural cues that facilitate continued fibroblast migration. Additionally, asiaticoside has been shown to promote fibroblast proliferation and cytoskeletal reorganization, further contributing to improved wound closure during the proliferative phase [73].

By Day 5, both hydrogels achieved complete wound closure, and no statistically significant difference was observed between the control and asiaticoside-loaded groups. This convergence suggests that while asiaticoside accelerates and sustains fibroblast migration, gelatin-based hydrogels alone are sufficient to support complete wound closure given adequate time. Similar findings have been reported in other *in vitro* and *in vivo* studies, where asiaticoside primarily enhanced the rate and quality of healing rather than altering the final extent of closure [74]. Importantly, the statistically significant improvement observed when comparing the Day 5 asiaticoside-treated group to the Day 1 control highlights the cumulative and time-dependent benefit of asiaticoside incorporation rather than a transient early-stage effect.

From a biomaterials perspective, these results support the potential application of asiaticoside-loaded gelatin hydrogels in wound healing and regenerative medicine. Sustained stimulation of fibroblast migration is particularly beneficial for chronic wounds, where impaired fibroblast activity is a major pathological feature. Recent studies incorporating asiaticoside into hydrogel-based delivery systems have demonstrated enhanced wound healing outcomes, further supporting the translational relevance of the present findings [75].

Overall, the scratch assay results demonstrate that asiaticoside incorporation into a gelatin-based hydrogel enhances fibroblast wound healing progression in a sustained and time-dependent manner. While both hydrogels ultimately supported complete wound closure, the asiaticoside-loaded formulation promoted prolonged fibroblast migratory activity, reinforcing its potential as a bioactive component for advanced wound healing applications.

Limitations and future directions

The focus of the current study is primarily on *in vitro* evaluation on the properties of the hydrogels and the impacts on cell viability. Although promising and valuable results were found, the same behaviour may not be properly reflected upon implementation on living organisms [21]. Consequently, the performance of these hydrogels *in vivo* remains an open question, which underscores the critical necessity of conducting studies in animal models, and later in clinical trials, to ascertain their long-term safety profile and therapeutic effectiveness. In addition, hemocompatibility assessment through haemolysis testing was not conducted in this study due to institutional ethical restrictions associated with the use of human or animal blood samples. Nevertheless, previous studies have reported that genipin-crosslinked gelatin-based hydrogels exhibit haemolysis ratios below the clinically acceptable threshold of 5%, indicating good blood

compatibility, while asiaticoside-containing biomaterials have also demonstrated favourable hemocompatibility in wound healing applications. Additionally, the cellular analysis in this work was conducted using only primary human dermal fibroblasts (HDFs) to measure the cytotoxicity of asiaticoside and to observe its effects on the rate of cell division. However, to achieve a more holistic understanding of asiaticoside's potential role in wound repair, future studies should include other pivotal cell types, such as keratinocytes and endothelial cells. This expansion would provide crucial insights into its performance regarding key biological processes like the restoration of the epithelial barrier (epithelialization) and the development of new blood supply.

Furthermore, although the investigation assessed fundamental physicochemical characteristics, including the swelling ratio, rate of biodegradation, and contact angle, it failed to account for external variables such as the potential for infection or the existence of diverse inflammatory mediators, both of which could significantly alter the hydrogel's performance within an actual wound environment. The degradation profile of the hydrogels was only examined over a brief timeframe, necessitating a more extended evaluation to fully comprehend the complete timeline of its breakdown. Either an overly rapid breakdown or an excessive persistence of the material at the wound site could negatively influence the process of healing and the regeneration of tissue. Finally, the research investigated the consequences of genipin crosslinking using only one specific concentration. A valuable next step would be to evaluate how different concentrations of genipin affect the hydrogel's mechanical properties and its level of cytotoxicity, as such an analysis would provide crucial insights for refining the formulation to achieve optimal performance for potential clinical applications [76].

Regarding future work, it is highly recommended to undertake *in vivo* studies to assess the performance of the gelatin-asiaticoside hydrogels within animal models [58,59]. Such research will be instrumental in determining the biocompatibility, effectiveness in promoting wound healing, and the long-term stability of these hydrogels in complex, living biological systems, with a particular focus on applications for chronic wound therapy. Following the acquisition of positive preclinical data, the progression to clinical trials with human subjects would be the logical next phase. These trials are necessary to yield vital information on the hydrogel's safety profile, therapeutic efficacy, and practical usability in actual clinical wound care settings, which would in turn inform any further optimization of the formulation. Ethics approval for the collection of blood samples will also be requested to enable haemolysis assay to be performed in this study moving forward. Conducting this assay will provide crucial information regarding the hemocompatibility of the biomaterials ink, ensuring that the formulations interaction with blood components is safe and further in depth understanding of the biomaterials ink to be used for wound healing application.

In addition, subsequent research could explore the integration of gelatin with other bioactive substances, for instance, chitosan, alginate, or silk fibroin. The inclusion of these materials holds the potential to further augment the hydrogel's mechanical robustness, biocompatibility, and its therapeutic wound healing capabilities [14]. Infection control is a critical factor in chronic wound management, and antibacterial performance is therefore an important functional requirement for wound-healing biomaterial ink. Although antibacterial efficiency was not directly evaluated in the present study, the antimicrobial relevance of the developed gelatin-asiaticoside hydrogels can be inferred from substantial existing literature. Asiaticoside has been reported to exhibit antibacterial activity against key wound-related pathogens such as *Staphylococcus aureus* and *Escherichia coli*, primarily through disruption of bacterial cell membranes and inhibition of microbial proliferation [58,77].

Importantly, asiaticoside loaded hydrogel and scaffold systems have demonstrated effective antibacterial performance in previous wound-healing studies. For example, injectable hydrogels incorporating asiaticoside have shown significant antibacterial activity and improved healing outcomes in infected wound models [77]. These findings suggest that incorporation of asiaticoside into a gelatin-genipin hydrogel matrix may contribute to infection control in addition to enhancing cytocompatibility and tissue regeneration. The present work was designed as an initial characterization study focusing on physicochemical properties, cytocompatibility, and printability of the biomaterial ink. Quantitative antibacterial evaluation will be included in future studies to further validate the antimicrobial performance of the formulation once required resources have been received.

Conclusion

Overall, gelatin-based hydrogels crosslinked with genipin and incorporated with asiaticoside have demonstrated significant potential for wound healing. The materials showed beneficial physicochemical features, including strong swelling ability, appropriate

biodegradation, and good hydrophilicity, all of which are advantageous for treating chronic wounds. The presence of asiaticoside also imparted additional antimicrobial and anti-inflammatory properties, which are vital for stimulating tissue repair and lowering infection risks.

Although the *in vitro* results are encouraging, further *in vivo* work is needed to confirm their long-term safety, biodegradation profile, and therapeutic effectiveness under clinical conditions. Incorporating advanced strategies such as 3D bioprinting and additional bioactive molecules may further enhance their performance and allow for personalized wound care. Future investigations that integrate stem cells, growth factors, or other therapeutic agents with these hydrogels could also accelerate healing and lead to better clinical outcomes.

Acknowledgments

All the authors would like to express our gratitude to the Department of Tissue Engineering and Regenerative Medicine, Faculty of Medicine, UKM for their guidance, and for providing the resources to complete this study.

Author contributions

Raniya Razif: Conceptualization, data curation, formal analysis, investigation, project administration, validation, visualization, writing – original draft and writing – review & editing; Andik Nisa Zahra Zainuddin: Formal analysis and writing – review & editing; Nurul Ain Zawawi: Formal analysis and writing – review & editing; Manira Maarof: Supervision, validation and writing – review & editing; Haslina Ahmad: Supervision, validation and writing – review & editing; Mohd Nor Fatimah: Supervision, validation and writing – review & editing; Mh Busra Fauzi: Conceptualization, data curation, formal analysis, funding acquisition, investigation, resources, supervision, validation, visualization, writing – original draft and writing – review & editing. All authors have read and agreed to the published version of the manuscript

Institutional review board statement

The study was conducted in accordance with the Declaration of Helsinki, and approved by the Universiti Kebangsaan Malaysia (UKM) Research Ethics Committee UKM (JEP-2024-904) (24102024).

Informed consent statement

The human skin samples were obtained from five consenting patients (written), and permission was obtained from each patient to publish their data.

Disclosure statement

No potential conflict of interest was reported by the authors.

Funding

The study was funded by grants provided by the Faculty of Medicine, Universiti Kebangsaan Malaysia under the Geran Fundamental Fakulti Perubatan (GFFP), grant code: FF-2024-447.

ORCID

Raniya Razif http://orcid.org/0009-0000-2018-2890
Andik Nisa Zahra Zainuddin http://orcid.org/0009-0004-6026-3483
Nurul Ain Zawawi http://orcid.org/0009-0004-4248-7264
Manira Maarof http://orcid.org/0000-0002-2154-7852
Haslina Ahmad http://orcid.org/0000-0002-0796-414X
Fatimah Mohd nor http://orcid.org/0000-0002-7126-5546
Mh Busra Fauzi http://orcid.org/0000-0001-6449-639X

Data availability statement

The original contributions presented in this study are included in the article. Further inquiries can be directed to the corresponding author.

References

[1] Loh EYX, Mohamad N, Fauzi MB, et al. Development of a bacterial cellulose-based hydrogel cell carrier containing keratinocytes and fibroblasts for full-thickness wound healing. Sci Rep. 2018;8(1):2875. doi:10.1038/s41598-018-21174-7.
[2] Han S-K. Basics of wound healing. In: Innovations and advances in wound healing. Springer Nature: Singapore; 2023. pp. 1–43. doi:10.1007/978-981-19-9805-8_1.
[3] Zawani M, Fauzi MB. Injectable hydrogels for chronic skin wound management: a concise review. Biomedicines. 2021;9(5):527. doi:10.3390/biomedicines9050527.
[4] Hoang TPN, Ghori MU, Ousey KJ, et al. Current and advanced therapies for chronic wound infection: an overview of chronic wounds, including their physiology, causes and management options. Pharm. J. 2022:309(7963). doi:10.1211/PJ.2022.1.148212.
[5] Kamolz LP, Lumenta DB, Kitzinger HB, et al. Tissue engineering for cutaneous wounds: an overview of current standards and possibilities. Eur Surg. 2008;40(1):19–26. European Surgery. doi:10.1007/s10353-008-0380-6.
[6] Ples M, Glik J, Misiuga M, et al. Chronic wounds and their treatment. Skin substitutes and allogeneic transplantations. J. Orthop. Trauma Surg. Relat. Res. 2016;1:28–36.
[7] Saeed S, Martins-Green M. Assessing animal models to study impaired and chronic wounds. Int J Mol Sci. 2024;25(7):3837. doi:10.3390/ijms25073837.
[8] Sizemore B, Singh K, Sen CK. A sociogenomic analysis of chronic wounds. IMPRS. 2022;5(1). doi:10.18060/27205.
[9] Lin C, Ailing H, Caifei LB, et al. Impact of symptoms on quality of life in patients with chronic wounds. Adv Skin Wound Care. 2024;37(11&12):1–9. doi:10.1097/asw.0000000000000219.
[10] Saifullah Q, Sharma A. Current trends on innovative technologies in topical wound care for advanced healing and management. Curr Drug Res Rev. 2024;16[M3]

[RR4(3):319–332. doi:10.2174/0125899775262048230925054922.
[11] Devdikar S, Reza A, Parsania T, et al. Analysis of efficacy of collagen dressing versus conventional dressing in chronic wound. IJAR. 2024;12(06):1249–1259. doi:10.21474/IJAR01/18989.
[12] Kulprachakarn K, Nantakool S, Rojawat C, et al. Effectiveness of combined conventional treatment with a tailored exercise training program on wound healing in patients with venous leg ulcer: a randomized controlled trial. J Tissue Viability. 2022;31(1):190–196. doi:10.1016/j.jtv.2021.06.010.
[13] Colin V, Listiana D. Efektivitas Perawatan Luka Dengan Metode Perawatan Luka Modern Dan Perawatan Luka Konvensional Pada Pasien Diabetes Melitus. JC. 2022;10(3):520–528. doi:10.33366/jc.v10i3.2112.
[14] Mahajan N, Soker S, Murphy SV. Regenerative medicine approaches for skin wound healing: from allografts to engineered skin substitutes. Curr Transpl Rep. 2024;11(4):207–221. doi:10.1007/s40472-024-00453-5.
[15] Zhang W, Liu W, Long L, et al. Responsive multifunctional hydrogels emulating the chronic wounds healing cascade for skin repair. J Control Release. 2023;354:821–834. doi:10.1016/j.jconrel.2023.01.049.
[16] Hu C, Liu W, Wang J, et al. Injectable hydrogels with tailored recombinant humanized collagen type I for the repair of damaged hearts by remodeling the myocardial microenvironment. Collagen & Leather. 2025;7(1):1–17. doi:10.1186/s42825-025-00212-x.
[17] Abuhamad AY, Masri S, Fadilah NIM, et al. Application of 3D-printed bioinks in chronic wound healing: a scoping review. Polymers. 2024;16(17):2456. doi:10.3390/polym16172456.
[18] Kim YS, Shin YS. Surface functionalization of 3D-printed bio-inspired scaffolds for biomedical applications: a review. Biomimetics. 2024;9(11):703. doi:10.3390/biomimetics9110703.
[19] Mandal A, Chatterjee K. The 3D/4D printing of polymeric scaffolds for bone tissue engineering. In Emerging materials and technologies for bone repair and regeneration. CRC Press: Boca Raton, FL, USA; 2024. pp. 85–108. doi:10.1201/9781003307310-6.
[20] Zhou X, Yu X, You T, et al. 3D printing-based hydrogel dressings for wound healing. Adv Sci (Weinh). 2024;11(47):e2404580. doi:10.1002/advs.202404580.
[21] Wang Y, Yuan X, Yao B, et al. Tailoring bioinks of extrusion-based bioprinting for cutaneous wound healing. Bioact Mater. 2022;17:178–194. doi:10.1016/j.bioactmat.2022.01.024.
[22] Yuan X, Zhu W, Yang Z, et al. Recent advances in 3D printing of smart scaffolds for bone tissue engineering and regeneration. Adv Mater. 2024;36(34):e2403641. doi:10.1002/adma.202403641.
[23] Zhai X, Wu Y, Tan H. Gelatin-based targeted delivery systems for tissue engineering. Curr Drug Targets. 2023;24(8):673–687. doi:10.2174/1389450124666230605150303.
[24] Kapoor D, Verma K, Jain S, et al. Gelatin-based hydrogels for drug delivery: a recent update. In Biomaterial-Based Hydrogels. Springer Nature: Singapore; 2024. pp. 66–87. doi:10.1007/978-981-99-8826-6_3.
[25] Wei Z, Zuo Y, Wu E, et al. Highly biocompatible, antioxidant and antibacterial gelatin methacrylate/alginate—Tannin hydrogels for wound healing. Int J Biol Macromol. 2024;279(Pt 4):135417. doi:10.1016/j.ijbiomac.2024.135417.
[26] Wahba MI. A comprehensive review on genipin: an efficient natural cross-linker for biopolymers. Polym Bull. 2024;81(16):14251–14305. doi:10.1007/s00289-024-05406-7.
[27] Ahmed R, Hira NUA, Wang M, et al. Genipin, a natural blue colorant precursor: Source, extraction, properties, and applications. Food Chem. 2024;434:137498. doi:10.1016/j.foodchem.2023.137498.
[28] Jovanović M, Petrović M, Stojanović D, et al. 3D-Printed Gelatin-Based Scaffold crosslinked by GenIPin: evaluation of mechanical properties and biological effect. Biopolymers. 2025;116(1):e23639. doi:10.1002/bip.23639.
[29] Scomazzon L, Ledouble C, Dubus M, et al. An increase in Wharton's jelly membrane osteocompatibility by a genipin-cross-link. Int J Biol Macromol. 2024;255:127562. doi:10.1016/j.ijbiomac.2023.127562.
[30] Masri S, Maarof M, Mohd NF, et al. Injectable cross-linked Genipin hybrid gelatin–PVA hydrogels for future use as bioinks in expediting cutaneous healing capacity: physicochemical characterisation and cytotoxicity evaluation. Biomedicines. 2022;10(10):2651. doi:10.3390/biomedicines10102651.
[31] Nike DU, Katas H, Mohd NF, et al. Characterisation of rapid in situ forming gelipin hydrogel for future use in irregular deep cutaneous wound healing. Polymers (Basel). 2021;13(18):3152. doi:10.3390/polym13183152.
[32] Fira N, Auliyah R, Rahmawati AU, et al. Effect of ethanol solution concentration in the extraction process of centella asiatica L. bioactive components using microwave-assisted extraction (MAE) method. J. Biobased Chem. 2022;2:113–125. doi:10.19184/jobc.v2i2.274.
[33] Orhan IE. Centella asiatica (L.) urban: from traditional medicine to modern medicine with neuroprotective potential. Evid.-Based Complement. Altern. Med. 2012;2012:1–8. doi:10.1155/2012/946259.
[34] Wankhade AM, Rahangdale PC. A review on centella asiatica: a potential herbal cure. Res. J. Pharmacogn. Phytochem. 2023;15:235–240. doi:10.52711/0975-4385.2023.00037.
[35] Bandopadhyay, S.; Mandal, S.; Ghorai, M.; Jha, N.K.; Kumar, M.; Radha, A.; Ghosh, A.; Proc'ków, J.; Pérez de la Lastra, J.M.; Dey, A. Therapeutic properties and pharmacological activities of asiaticoside and madecassoside: A review. J Cell Mol Med, 52023, 27, 593–608. doi:10.1111/jcmm.17635.
[36] He Z, Hu Y, Niu Z, et al. A review of pharmacokinetic and pharmacological properties of asiaticoside, a major active constituent of Centella asiatica (L.) Urb. J Ethnopharmacol. 2023;302(Pt A):115865. doi:10.1016/j.jep.2022.115865.
[37] Abdul Ghani NI, Maarof M, Roy Chowdhury S, et al. Effect of dermal fibroblast conditioned medium on keratinocytes irrespective of age group. JSM. 2023;52(1):223–231. doi:10.17576/jsm-2023-5201-18.
[38] Ouyang L, Yao R, Zhao Y, et al. Effect of bioink properties on printability and cell viability for 3D bioplotting of embryonic stem cells. Biofabrication. 2016;8(3):035020. doi:10.1088/1758-5090/8/3/035020.
[39] Ribeiro A, Blokzijl MM, Levato R, et al. Assessing bioink shape fidelity to aid material development in 3D bio-

printing. Biofabrication. 2017;10(1):014102. doi:10.1088/1758-5090/aa90e2.
[40] Salleh A, Mustafa N, Teow YH, et al. Dual-layered approach of ovine collagen-gelatin/cellulose hybrid biomatrix containing graphene oxide-silver nanoparticles for cutaneous wound healing: fabrication, physicochemical, cytotoxicity and antibacterial characterisation. Biomedicines. 2022;10(4):816. doi:10.3390/biomedicines10040816.
[41] Loh QL, Choong C. Three-dimensional scaffolds for tissue engineering applications: role of porosity and pore size. Tissue Eng Part B Rev. 2013;19(6):485–502. doi:10.1089/ten.TEB.2012.0437.
[42] Sharifi E, Sadati SA, Yousefiasl S, et al. Cell loaded hydrogel containing Ag-doped bioactive glass-ceramic nanoparticles as skin substitute: Antibacterial properties, immune response, and scarless cutaneous wound regeneration. Bioeng Transl Med. 2022;7(3):e10386. doi:10.1002/btm2.10386.
[43] Wu P, Fisher A, Foo P, et al. In vitro assessment of water vapour transmission of synthetic wound dressings. Biomaterials. 1995;16(3):171–175. doi:10.1016/0142-9612(95)92114-l.
[44] Zawawi NA, Maarof M, Fadilah NIM, et al. Hybrid adhesive hydrogel patch containing genipin-crosslinked gelatin–hyaluronic acid for future use in atopic dermatitis. J Funct Biomater. 2025;16(6):195. doi:10.3390/jfb16060195.
[45] Masri S, Maarof M, Aziz IA, et al. Performance of hybrid gelatin-PVA bioinks integrated with genipin through extrusion-based 3D bioprinting: An in vitro evaluation using human dermal fibroblasts. Int J Bioprint. 2023;9(3):677. doi:10.18063/ijb.677.
[46] Cohen J. Statistical power analysis for the behavioral sciences. (2nd ed.); Routledge. New York. 2013. doi:10.4324/9780203771587.
[47] Nizam AAK, Md Fadilah NI, Ahmad H, et al. Injectable gelatin-palmitoyl-GDPH hydrogels as bioinks for future cutaneous regeneration: physicochemical characterization and cytotoxicity assessment. Polymers (Basel). 2024;17(1):41. doi:10.3390/polym17010041.
[48] Yuliati L, Mardliyati E, Bramono K, et al. Asiaticoside induces cell proliferation and collagen synthesis in human dermal fibroblasts. UnivMed. 2015;34(2):96. doi:10.18051/UnivMed.2015.v34.96-103.
[49] Shen H, Zhu F, Li J, et al. Protective effect of asiaticoside on radiation-induced proliferation inhibition and DNA damage of fibroblasts and mice death. Open Life Sci. 2020;15(1):145–151. doi:10.1515/biol-2020-0015.
[50] Gong H, Yang L, Li Y, et al. Metal-polyphenol nanocomposite hybrid hydrogel: a multifunctional platform for treating diabetic foot ulcers through metabolic microenvironment reprogramming. Biomaterials. 2025;322:123414. (. doi:10.1016/j.biomaterials.2025.123414.
[51] Mahmoudi C, Tahraoui Douma N, Mahmoudi H, et al. Developing and characterizing a biocompatible hydrogel obtained by cross-linking gelatin with oxidized sodium alginate for potential biomedical applications. Polymers (Basel). 2024;16(22):3143. doi:10.3390/polym16223143.
[52] Milano F, Masi A, Madaghiele M, et al. Current trends in gelatin-based drug delivery systems. Pharmaceutics. 2023;15(5):1499. doi:10.3390/pharmaceutics15051499.
[53] Biochemical assay reagent. ; n.d.). Invivochem.com. Retrieved January 17, 2026, from https://www.invivochem.com/gelatins.html.
[54] Alorbu C, Cai L. Fungal resistance and leachability of genipin-crosslinked chitosan treated wood. International Biodeterioration & Biodegradation. 2022;169(:105378. doi:10.1016/j.ibiod.2022.105378.
[55] Ahmed SR, Rabbee MF, Roy A, et al. Therapeutic promises of medicinal plants in bangladesh and their bioactive compounds against ulcers and inflammatory diseases. Plants (Basel). 2021;10(7):1348. doi:10.3390/plants10071348.
[56] Weng T, Zhang W, Xia Y, et al. 3D bioprinting for skin tissue engineering: current status and perspectives. J Tissue Eng. 2021;12:20417314211028574. doi:10.1177/20417314211028574.
[57] Arif MMA, Fauzi MB, Nordin A, et al. Fabrication of bio-based gelatin sponge for potential use as a functional acellular skin substitute. Polymers (Basel). 2020;12(11):2678. doi:10.3390/polym12112678.
[58] Razif R, Fadilah NIM, Ahmad H, et al. Asiaticoside-loaded multifunctional bioscaffolds for enhanced hyperglycemic wound healing. Biomedicines. 2025;13(2):277. doi:10.3390/biomedicines13020277.
[59] Razif R, Fadilah NIM, Maarof M, et al. Physicochemical characterization of injectable genipin-crosslinked gelatin–kelulut honey hydrogels for future cutaneous tissue loss. Polymers (Basel). 2025;17(9):1129. doi:10.3390/polym17091129.
[60] Lin N, Zuo B. Silk sericin/fibroin electrospinning dressings: a method for preparing a dressing material with high moisture vapor transmission rate. J Biomater Sci Polym Ed. 2021;32(15):1983–1997. doi:10.1080/09205063.2021.1952383.
[61] Amirrah IN, Lokanathan Y, Zulkiflee I, et al. A comprehensive review on collagen type i development of biomaterials for tissue engineering: from biosynthesis to bioscaffold. Biomedicines. 2022;10(9):2307. doi:10.3390/biomedicines10092307.
[62] Hoffman AS. Hydrogels for biomedical applications. Adv Drug Delivery Rev. 2012;64:18–23. doi:10.1016/j.addr.2012.09.010.
[63] Liang Y, He J, Guo B. Functional hydrogels as wound dressing to enhance wound healing. ACS Nano. 2021;15(8):12687–12722. doi:10.1021/acsnano.1c04206.
[64] Stojkov G, Niyazov Z, Picchioni F, et al. Relationship between structure and rheology of hydrogels for various applications. Gels. 2021;7(4):255. doi:10.3390/gels7040255.
[65] Samimi Gharaie S, Dabiri SMH, Akbari M. Smart shear-thinning hydrogels as injectable drug delivery systems. Polymers (Basel). 2018;10(12):1317. doi:10.3390/polym10121317.
[66] Liu J, Liu Y, Brown EM, et al. Development and characterization of genipin cross-linked gelatin based composites incorporated with vegetable-tanned collagen fiber (VCF). JALCA. 2017;116(10):310–319. doi:10.34314/jalca.v116i10.4616.
[67] Ho T-C, Chang C-C, Chan H-P, et al. Hydrogels: properties and applications in biomedicine. Molecules. 2022;27(9):2902. doi:10.3390/molecules27092902.
[68] Ilkar Erdagi S, Asabuwa Ngwabebhoh F, Yildiz U. Genipin crosslinked gelatin-diosgenin-nanocellulose hydrogels for potential wound dressing and healing applications. Int J Biol Macromol. 2020;149:651–663. doi:10.1016/j.ijbiomac.2020.01.279.
[69] Tahri S, Maarof M, Masri S, et al. Human epidermal keratinocytes and human dermal fibroblasts interactions

seeded on gelatin hydrogel for future application in skin in vitro 3-dimensional model. Front Bioeng Biotechnol. 2023;11:1200618. doi:10.3389/fbioe.2023.1200618.

[70] Atef AK, Mostafa TB, El-Sherif HM. Hemocompatible gelatin-glycidyl methacrylate/graphene oxide composite hydrogels for vascular catheter applications. Sci Rep. 2025;15(1):10224. doi:10.1038/s41598-025-93040-2.

[71] Wang H, Li Q, Jiang Y, et al. Functional hydrogels with chondroitin sulfate release properties regulate the angiogenesis behaviors of endothelial cells. Gels. 2022;8(5):261. doi:10.3390/gels8050261.

[72] Tolabi H, Haghbin Nazarpak M, Solouk A, et al. 3D printing of genipin crosslinked alginate/gelatin Ink for tissue engineering application. Int J Biol Macromol. 2025;329(Pt 1):147839. doi:10.1016/j.ijbiomac.2025.147839.

[73] Suriyah WH, Rizal AJ, Nadzirin HSM, et al. *In vitro* wound healing effect of asiaticoside extracted from *Centella asiatica* ("Pegaga") on human gingival fibroblast cell line. MSF. 2021;1025:224–229. doi:10.4028/www.scientific.net/msf.1025.224.

[74] Narisepalli S, Salunkhe SA, Chitkara D, et al. Asiaticoside polymeric nanoparticles for effective diabetic wound healing through increased collagen biosynthesis: in-vitro and in-vivo evaluation. Int J Pharm. 2023;631:122508. doi:10.1016/j.ijpharm.2022.122508.

[75] Witkowska K, Paczkowska-Walendowska M, Plech T, et al. Chitosan-based hydrogels for controlled delivery of asiaticoside-rich centella asiatica extracts with wound healing potential. Int J Mol Sci. 2023;24(24):17229. doi:10.3390/ijms242417229.

[76] Gadge AS, Shirsat DV, Soumia PS, et al. Physiochemical, biological, and therapeutic uses of stingless bee honey. Front Sustain Food Syst. 2024;7:1324385. doi:10.3389/fsufs.2023.1324385.

[77] Chonsut P, Romyasamit C, Konyanee A, et al. Potential activities of *Centella asiatica* leaf extract against pathogenic bacteria-associated biofilms and its anti-inflammatory effects. Adv Pharmacol Pharm Sci. 2024;2024(1):5959077. doi:10.1155/2024/5959077.